PATTERN FORMATION IN COUPLED NETWORKS WITH INHIBITION AND GAP JUNCTIONS

by

Fatma Gürel Kazancı

B.S. Mathematics, Middle East Technical University, 2000

Submitted to the Graduate Faculty of

the School of Arts and Sciences in partial fulfillment

of the requirements for the degree of

Doctor of Philosophy

University of Pittsburgh

2007

UNIVERSITY OF PITTSBURGH

SCHOOL OF ARTS AND SCIENCES

This dissertation was presented

by

Fatma Gürel Kazancı

It was defended on

January 30

and approved by

G. Bard Ermentrout, Department of Mathematics

Jonathan Rubin, Department of Mathematics

William Troy, Department of Mathematics

Nathan Urban, Department of Biological Sciences, CMU

Dissertation Director: G. Bard Ermentrout, Department of Mathematics

_____ G. Bard Ermentrout, Dissertation Director

PATTERN FORMATION IN COUPLED NETWORKS WITH INHIBITION AND GAP JUNCTIONS

Fatma Gürel Kazancı, PhD

University of Pittsburgh, 2007

In this dissertation we analyze networks of coupled phase oscillators. We consider systems where long range chemical coupling and short range electrical coupling have opposite effects on the synchronization process. We look at the existence and stability of three patterns of activity: synchrony, clustered state and asynchrony.

In Chapter 1, we develop a minimal phase model using experimental results for the olfactory system of Limax. We study the synchronous solution as the strength of synaptic coupling increases. We explain the emergence of traveling waves in the system without a frequency gradient. We construct the normal form for the pitchfork bifurcation and compare our analytical results with numerical simulations.

In Chapter 2, we study a mean-field coupled network of phase oscillators for which a stable two-cluster solution exists. The addition of nearest neighbor gap junction coupling destroys the stability of the cluster solution. When the gap junction coupling is strong there is a series of traveling wave solutions depending on the size of the network. We see bistability in the system between clustered state, periodic solutions and traveling waves. The

bistability properties also change with the network size. We analyze the system numerically and analytically.

In Chapter 3, we turn our attention to a very popular model about network synchronization. We represent the Kuramoto model in its original form and calculate the main results using a different technique. We also look at a modified version and study how this effects synchronization. We consider a collection of oscillators organized in m groups. The addition of gap junctions creates a wave like behavior.

TABLE OF CONTENTS

LIST OF FIGURES

PREFACE

I would like to thank the members of my thesis committee, Prof. Troy, Prof. Rubin and Prof. Urban. I learned a great deal from Prof. Troy and Prof. Rubin during the classes I have taken with them. Their contribution to my education process is invaluable.

I also thank Prof. Riviere, Prof. Hastings, Prof. Yotov and Prof. Lennard for their guidance throughout the years. It is an honor to be a student in any of your classes. My special thanks also goes to Ms. Cathy Duane-Lennard, I was honored to work with you.

I am in debt to my Ph.D advisor, Prof. Bard Ermentrout for everything I have learned from him. I wish that this process never ends and hopefully we continue collaborating in the future. I will miss his teaching style, jokes and more than ever his never ending energy and hunger for science. I thank him for introducing to me to this field and for supporting me during my education in many ways.

I would also like to thank the wonderful staff of the Math Department, especially Drew Porvaznik and Molly Williams for helping me with all the little details along my studentship.

I thank all my student friends at Pitt. Special thanks goes to Monika and Alfy (survivors from class of 2001); fellow fifth floor residents Angela, Jyotsna, Carolina and Evandro for the lovely conversations and their friendship; ex-Pitt students Lerna, Atife, Songul, Huseyin and Meryem for the comfort of conversing in Turkish and good food; and my dear officemates:

Stephanie, Aushra and Jon for maintaining a peaceful study environment and for their friendship. Thanks for all the good times. You will be missed greatly.

I would like to extend my many thanks to my family, my mom, dad, brothers, sisters, nieces, nephews, extended family and my friends both from Pittsburgh and Turkey. Your love, support and prayers keeps me going. Last but not least, I would like to thank my husband, Caner, for always supporting me, helping me whenever I needed help and always being there for me. I couldn't have done it without you.

I would like to dedicate my thesis to the memory of my grandfather Mashar Erol who passed away in 2000. He would have been very happy to see this day.

1.0 INTRODUCTION

Study of the human brain has been the interest of researchers for centuries. The anatomy of human brain is fairly well-known. This vast complex contains more than one hundred billion neurons which are connected to other neurons via electrical and/or chemical synapses. Advances in experimental methods and imaging techniques enabled researchers to learn the architecture in different areas of the brain. However, there is still a long way to go before we fully understand how the brain functions and generates various rhythms. Collaboration among scientists from both experimental and theoretical backgrounds is needed to solve this big puzzle. Mathematical modeling is useful in combining the physiological information and neural function. Models developed for specific areas help us gain insight into how that particular part works and hopefully leads us to theories that are applicable to similar systems.

For computational purposes, neurons can be considered as intrinsic oscillators. Each neuron is coupled to others via electrical and/or chemical synapses. Often times when we try to model a system, we have limited information about the parameters. We also want to make a model that is small enough so that we can perform efficient numerical simulations or mathematically analyze it but large enough to capture the important features of the system. We will use phase models to represent the systems we study. These models can be used to explain biophysical data showing synchronization in areas of brain, wave activity or

formation of other stable patterns of activity.

Oscillations are seen throughout the nervous system ranging from slow oscillations (< 5 Hz) observed during sleep to fast oscillations (> 20 Hz) that are associated with seizures. Coupled oscillators are used to model central pattern generators that are responsible for locomotion. There are several patterns we can observe in an oscillatory networks such as synchrony, asynchrony, clusters and traveling waves. Definition of synchrony can be ambiguous. We say that the network is synchronized when the oscillators are both frequency and phase locked. In-phase synchrony means that there is no difference between individual phases. Asynchrony is the state where phases of the oscillators are distributed on $\mathbb{S}^1$. When coupling is strong enough, this solution tends to lose stability. A clustered state is observed when oscillators are organized in groups and within the group, there is no phase difference. As the number of the clusters increase it gets harder for the clustered solution to be stable. Traveling waves can be categorized as phase-locked solutions as the phase differences don't change but the individual phases do as time evolves.

Networks of coupled neural oscillators exhibit a variety of activity patterns depending on the properties of the coupling. There is clear experimental evidence for the existence of electrical and chemical synapses in neocortical inhibitory networks [26]. The effect of each type of coupling in isolation is well-studied. Depending on the nature of the neural oscillation, inhibition can be either synchronizing or desynchronizing. van Vreeswijk et al. showed that with non-instantaneous synapses, inhibition can synchronize a network [56]. On the other hand, Kopell and Ermentrout used a model network where long distance inhibitory coupling favored anti-phase behavior between two mutually coupled oscillators [17]. Electrical coupling between oscillators is established via gap junctions. In numerous computational and

theoretical studies, it has been shown that electrical coupling can either promote synchrony or anti-synchrony [55, 5, 8], depending on the shape of the action potential and the nature of the oscillator. For example, in the presence of CBX, a blocker for electrical synapses, Bou-Flores and Berger report that they have seen more synchronized activity in a network of inspiratory motoneurons [6].

Recently, the combined effects of these couplings have been an area of theoretical interest [46, 42, 4, 49]. In these papers, both the inhibition and the gap junctions encouraged synchronization. Coupling was between pairs of oscillators or in all-to-all coupled networks.

In this thesis, we investigate pattern formation in a network of coupled neurons with both types of coupling. Throughout the thesis, we look at the case where chemical coupling has desynchronizing effects and electrical coupling has synchronizing effects. There are different ways to look at the spatial interactions between synchronizing and anti-synchronizing influences. The equations we are interested can be written as:

$$\frac{d\theta_j}{dt} = \frac{1}{N}\sum_{k=1}^{N} H_{syn}(\theta_k - \theta_j) + \sum_{l=-m}^{m} w_l H_{gap}(\theta_{j+l} - \theta j)$$

where $w_l = w_{-l}$ are non-negative and H_{syn}, H_{gap} are T- periodic in their argument. m represents the scope of gap junctions. For simplicity, we will work in a ring of oscillators to avoid boundary effects. The function H_{syn} favors the anti-phase state for pairwise interactions so that $T/2$ is a stable fixed point for a pair. Similarly, H_{gap} favors synchrony. We imagine H_{syn} is synaptic coupling and H_{gap} is gap junctional so that the former are long range and the latter local. We show that $\theta_j = \Omega t + 2\pi nj/N$ is a solution for the system given above for a correctly chosen Ω.

In Chapter 1, we derive a phase model from a biophysical model for neurons in the olfactory lobe of Limax. The model has the form given above. We show that synchrony

($n = 0$) and traveling wave ($n = 1$) are solutions to this system. We determine their stability as the system parameters change. Normal form for the bifurcation from synchrony is calculated. Our analytical results are justified using numerical simulations. This part of the thesis has recently appeared in a scientific journal [29].

In Chapter 2, we investigate the possibility of clustered solutions in a system with similar structure to the one studied in Chapter 1. The only difference is the scope of the gap junctions is restricted to only nearest neighbors. We see that the system supports a stable two-cluster solution when the strength of local gap junction coupling is small. For larger values of gap junction coupling, the traveling wave solution is stable. We go through linear stability analysis and compute the bifurcation diagrams numerically. We show that the system exhibits bistability in some regions for the bifurcation parameter. We are in the process of writing a paper on our findings for this section.

In Chapter 3, we take another approach and study the stability of asynchronous solution. We first review the Kuramoto Model. We extend the Kuramoto model to include local coupling between oscillators. We are able to generalize the results found in previous chapters. We also present a different way of computing the critical coupling strength for transition from asynchrony to a synchronous solution. This chapter serves as a step for future research as the work presented is preliminary.

2.0 SYNCHRONY AND TRAVELING WAVES

2.1 INTRODUCTION

In most of theoretical studies, neurons are represented as oscillators. About 30 years ago, studying coupled oscillators in a system with more than two oscillators was almost impossible. Arthur Winfree argued that a system with an asymptotically stable limit cycle attractor can be represented using only one variable: the phase of the oscillator on the limit cycle [59]. An autonomous differential equation is said to have an asymptotically stable limit cycle if the perturbations from the limit cycle solution returns to the oscillation as $t \to \infty$. There may be a shift in the time course due to time-translation invariance of the periodic solution. The periodic trajectory remains unchanged by translation in time. For an oscillator with period T, we identify $t = 0$ with the time of peak value for the oscillating variable and we return to the same value at $t = T$ [50]. Specifying the time coordinate, we are able to define the phase of the periodic solution. Once the reference point is chosen, the phase can be defined uniquely.

For the uncoupled system, no additional information about the intrinsic properties of the oscillators is needed to use the phase model for representing the system. In the case of a coupled system, where the coupling is weak enough, we can use a similar formulation

to represent the network by a phase model where the interactions between the oscillators is represented through phase differences. Details of the theory can be found in [60, 44, 34, 38]. This was suggested by Arthur Winfree, proven by John Guckenheimer and has been used by Neu, Kuramoto, Ermentrout, Kopell and many others over the years [25, 28, 43, 47].

Our aim in this chapter is to explore what happens in spatially distributed networks when one form of coupling (here, electrical coupling via gap junctions) encourages synchrony but the other form of coupling (synaptic inhibition) encourages, at least pairwise, anti-phase locking. More specifically, we suppose that the synchronous coupling is local and the desynchronizing coupling is long range. Since electrical junctions require that membranes of the cells to be in direct contact, we expect that gap junction coupling is spatially localized. In contrast, chemical inhibition might be expected to have longer range. We study the bifurcation to patterns in a general network of oscillators with long range desynchronizing coupling and short range synchronizing coupling. The strength of the former coupling is a parameter which when increased causes the synchronous state to lose stability. We determine the critical values for this parameter via linear stability analysis and the direction of the bifurcation via a normal form calculation. To make the analysis possible and to avoid the confound of boundary effects, we forgo the linear chain and work on a circular domain. Numerical results of the chain produce similar behavior, but the analysis is considerably more difficult. The normal form calculation is made somewhat more difficult by the presence of a zero eigenvalue arising from translation invariance. Our method is to first reduce the biophysical model that serves as our motivation to a chain of phase-coupled oscillators on which we can apply the general theory. Thus, in the first section, after introducing the biophysical model, we compute the interaction functions under the assumption of weak

coupling. We show that for this model, gap junctions are synchronizing while chemical inhibition is desynchronizing. Next, we analyze the bifurcation of patterned states from synchrony in a continuum chain of phase-oscillators. We find a novel phase-locked state which is patterned but not a traveling wave. We numerically illustrate the transition to traveling waves as predicted in the reduced system and provide conditions for the stability of the traveling wave.

2.2 MOTIVATION: LIMAX MODEL

In a series of papers, Ermentrout et al. explored oscillations and waves in the olfactory lobe of *Limax maximus* [15, 13]. Our motivation comes from their work: we provide mathematical analysis for the activity patterns they have observed in this particular system and extend it to more general systems.

In the first paper they use a minimal phase model to describe the network, whereas in the last paper they propose a conductance-based model. Since little is known about the currents responsible for the generation of the oscillations, we return to using a phase model but we compute the interaction functions using the conductance-based model. Phase models have proven to be useful tools when the biophysical properties of the cells and/or the synaptic interactions between cells are not well known. They have been successfully implemented in explaining experimental results such as for the lamprey swim CPG [58]. Transition from a biophysical model for the uncoupled neurons to a phase model can be done when the original system has an asymptotically stable limit cycle solution. When we consider the case of weak coupling a similar transition allows us to represent the system in terms of phase

differences. Details of the theory behind phase models and weak coupling can be found in [34]. Statements of the main theorems are given in Appendix A.

In [13], Ermentrout et al. describe a model network that consists of a spatially distributed network of bursting and non-bursting cells. They arrange each type of cell on a one-dimensional array that consists of 21 cells. Each bursting cell receives nearest neighbor gap-junction coupling, equal coupling through inhibition from 5 neighbors on each side and synaptic excitation from the local non-bursting cell. Each non-bursting cell receives local inhibition from the bursting cell and recurrent excitation from 3 neighbors on each side. When only a single bursting cell is considered, oscillatory behavior can be seen. The dynamics of a single bursting cell is given by three currents: leak, potassium and T-type calcium. They take a gradient for the leak potential, $E_{leak} = -80$ mV at the apical end and $E_{leak} = -83$ mV at the basal end. The frequency of oscillations vary from 0.8 to 1.5 Hz. Figure (2.2.1) represents the oscillations when $E_{leak} = -82$ mV.

In the Limax model, the inhibition is global in that each cell inhibited all the other cells in the network while the gap junctions were only between nearest neighbors. We show below, that inhibition is desynchronizing for the slug model and that gap junctions synchronize, so the slug model serves as an example of a spatially distributed network in which the two types of coupling work in opposition. Ermentrout and Kopell [17] explored the effects of one or two long range desynchronizing interactions between cells that were coupled with local synchronizing interactions. Various types of waves were found via direct analytic calculations which were possible due to the simple form of the coupling. There are several mechanisms for wave propagation in coupled neural networks. One mechanism is having a pacemaker-like region that generates the wave. Another mechanism is to have a frequency gradient,

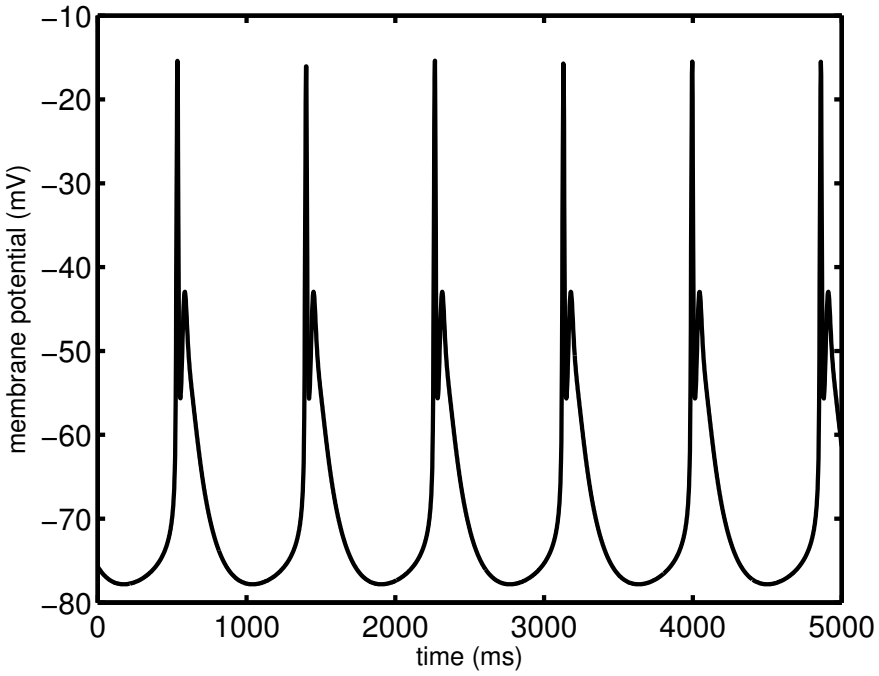

Figure 2.2.1: Uncoupled bursting cells oscillate with a frequency ranging from 0.8 Hz to 1.5 Hz depending on the value of leak potential. Here $E_{leak} = -82$ mV and the period of the oscillations is about 860 ms.

like we have in the above system. Under resting conditions the Limax lobe produces slow periodic traveling waves of electrical activity. Experimentally, the wave of activity is biased to move in one direction because of an intrinsic gradient in the frequency of the bursting cells. Furthermore, the authors discovered that even in the absence of a gradient in frequency, it was possible to generate waves in an otherwise homogeneous network. With large enough gap junction coupling (or small enough inhibition), the network synchronized. However, with weak electrical coupling the network becomes desynchronized, breaking into clusters of cells with different phase-lags. At intermediate coupling strengths, the network produces waves.

2.3 THE BIOPHYSICAL MODEL AND REDUCTION

The biophysical model introduced in [13] consists of bursting and non-bursting cells in the procerebral lobe of Limax. The bursting cells oscillate at about 1 Hz and are responsible for the electrical wave observed in the lobe. The nonbursting cells fire only in the presence of extrinsic stimuli. Thus, since we are only interested in the genesis of the wave, we focus on the bursting cells. Each cell is an intrinsic oscillator and, in the model, two types of synapses coupled the oscillating neurons: chemical inhibition and electrical or gap junctions. The membrane potential for each bursting cell obeys the following equations:

$$C\frac{dV}{dt} = -I_L - I_K - I_{Ca} - I_{gap} - I_{syn}$$

where each term is a current due respectively to the leak, the potassium channels, the calcium channels, the gap junction coupling, and the synaptic inhibition. We used the parameters

given in Appendix A. The gap junction coupling is over nearest neighbors and depends on the voltage difference between the pre and post-synaptic cells:

$$I_{gap} = g_{gap}(V_{post} - V_{pre}).$$

Here, "post" refers to the cell receiving the connection from "pre" cell. The inhibition, I_{syn} is global - every cell inhibits every other cell. Each synaptic interaction adds a current of the form:

$$I_{syn} = g_{syn} s_{pre}(V_{post} - E_{syn})$$

where $E_{syn} = -78$ mV and the synaptic conductance obeys an equation of the form

$$\frac{ds_{pre}}{dt} = 0.1/(1 + \exp(-(V_{pre} + 45)/5)) - s_{pre}/100.$$

Networks of coupled oscillators are generally difficult to analyze. However, the method of averaging has proven to be very useful for studying synchronization between oscillators [49]. That is, if we assume that the conductances g_{gap}, g_{syn} are sufficiently small, it is possible to reduce a network of coupled oscillators to a system of phase models where each oscillator is represented by its scalar phase and interactions are through the differences in the phases [59, 44, 25]. Let V_i be the membrane potential of the ith cell and s_i be the synaptic component of the ith cell. If

$$-I_{syn,i} = -g_{syn} \sum_j w_{ij} s_j (V_i - E_{syn})$$

is the synaptic current into the ith cell and w_{ij} is the weight of the connection between cell i and j, which is taken to be $1/N$ where N is the number of oscillators, then with the weak coupling assumption, the phase interactions will take the form:

$$-\bar{I}_{syn,i} = g_{syn} \sum_j w_{ij} H_{syn}(\theta_j - \theta_i) \tag{2.1}$$

where

$$H_{syn}(\phi) = \frac{1}{T}\int_0^T V^*(t)s(t+\phi)(E_{syn} - V(t))\ dt.$$

$V^*(t)$ is the voltage component for the $T-$periodic solution to the adjoint equation for the stable limit cycle. $V(t)$, $s(t)$ are the voltage and synaptic components respectively. For the gap junction coupling, we find:

$$-\bar{I}_{gap,i} = g_{gap}\sum_j z_{ij}H_{gap}(\theta_j - \theta_i) \tag{2.2}$$

where

$$H_{gap}(\phi) = \frac{1}{T}\int_0^T V^*(t)(V(t+\phi) - V(t))\ dt.$$

The weights, z_{ij}, satisfy $z_{ij} = f(|i-j|)$ where f is a decreasing function in its argument. The phase of each oscillator, θ_i obeys the reduced dynamics:

$$\theta_i' = 1 - \bar{I}_{syn,i} - \bar{I}_{gap,i}$$

where the two currents are given by equations (2.1) and (2.2). The phase of each oscillator maps directly onto the potential (or other oscillating variable for the system) of each bursting cell once the zero phase is chosen. A standard choice of zero phase is the peak of the membrane potential.

Figure 2.3.1 shows both H_{syn} and H_{gap} for the Limax model evaluated numerically using XPPAUT [22] along with their approximations using the 0, 1, 2 order terms of the Fourier expansion. The Fourier approximations of these functions are used in the remaining part of this chapter. They can be found in Appendix A. Note that, $H_{syn}(0) \neq 0$, $H_{gap}(0) = 0$, $H'_{syn}(0) < 0$, and $H'_{gap}(0) > 0$ for the functions graphed in Figure 2.3.1.

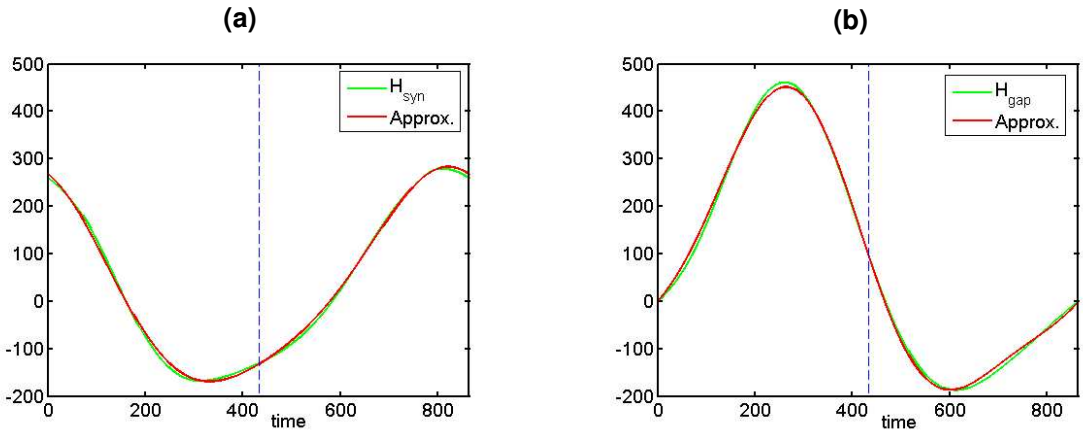

Figure 2.3.1: Coupling functions are computed using XPPAUT. Approximations are estimated from the Fourier expansion. (a) shows H_{syn} and its approximation and (b) shows H_{gap} and its approximation. The functions are plotted over a period of the oscillations and the dashed blue line marks half period.

To interpret the meaning of these inequalities, consider a pair of identical cells:

$$\begin{aligned}\theta_1' &= 1 + g_{syn}H_{syn}(\theta_2 - \theta_1) + g_{gap}H_{gap}(\theta_2 - \theta_1)\\ \theta_2' &= 1 + g_{syn}H_{syn}(\theta_1 - \theta_2) + g_{gap}H_{gap}(\theta_1 - \theta_2).\end{aligned}$$

Let $\phi = \theta_2 - \theta_1$. Then

$$\phi' = g_{syn}[H_{syn}(-\phi) - H_{syn}(\phi)] + g_{gap}[H_{gap}(-\phi) - H_{gap}(\phi)] \equiv F(\phi).$$

Phase-locked states for this first order equation are those where ϕ does not change, i.e. the phase difference between the two oscillators is fixed. They are roots of the function $F(\phi)$ and they are stable if $F'(0) < 0$. Clearly, $F(\phi)$ is the sum of odd parts of the functions H_{syn} and H_{gap}. Since any odd periodic function has at least two fixed point, $\phi = 0$ and $\phi = T/2$, there will always exist phase-locked states. These may not be the only phase-locked solutions and the stability has to be determined for the particular choice of interaction functions. Synchronous solution ($\phi = 0$) imply that both membranes fire together. In our case, the stability condition for synchrony is as follows:

$$g_{syn}H'_{syn}(0) + g_{gap}H'_{gap}(0) > 0.$$

Since the conductances, g_{syn}, g_{gap} are non-negative, $H'_{syn}(0) < 0$ and $H'_{gap}(0) > 0$, synchrony is stable if the gap junctions dominate. Anti-phase solutions ($\phi = T/2$) are exactly one cycle apart. This anti-phase solution will be stable for the coupled pair if $F'(T/2) < 0$ or equivalently

$$g_{syn}H'_{syn}(T/2) + g_{gap}H'_{gap}(T/2) > 0.$$

As seen in Figure 2.3.1 by the dashed vertical lines at $T/2$, anti-phase is stable for synaptic and unstable for gap junction coupling. In the models considered by Lewis and Rinzel, both

synaptic and electrical coupling encourage stable synchrony [46]. Thus, the interaction of networks will lead to synchronous behavior. In contrast, for the intrinsic dynamics in the Limax model, electrical coupling encourages synchrony but synaptic inhibition opposes it. Our goal in the rest of this chapter is to explore the consequences of these differences in a one-dimensional spatially organized array of N oscillators.

2.3.1 The spatial equations

We introduce a discrete model where we have all-to-all synaptic coupling and local gap junction coupling. The equations can be written down as

$$\frac{d\theta_j}{dt} = \omega + \frac{g_{syn}}{N}\sum_{k=1}^{N} H_{syn}(\theta_k - \theta_j) + g_{gap}\sum_{\ell=-m}^{m} J_\ell H_{gap}(\theta_{j+\ell} - \theta_j), \quad \text{j=1,}\ldots,N \tag{2.3}$$

where θ_j represents the phase of oscillator j, ω is the intrinsic frequency for all the oscillators, g_{syn} is the synaptic coupling strength , g_{gap} is the strength of electrical coupling and H_{syn}, H_{gap} are the functions describing synaptic and gap junction coupling , respectively. We note that the key point in the weak coupling assumption is that the effects of different types of coupling are linear and additive. Thus, only the ratio of g_{syn} and g_{gap} in the phase model matter. The factor $\frac{1}{N}$ in front of the synaptic coupling contribution guarantees that the model also works when we allow $N \to \infty$. The weights J_ℓ are taken to be non-negative and we assume that $J_{-\ell} = J_\ell$. m represents the scope of gap junction coupling. We also note that $m << N$, since we assume gap junction coupling is local. Henceforth, we assume the period of the oscillators (and thus of the coupling functions) is 2π. The function H_{syn} favors the anti-phase state for pairwise interactions so that π is a stable fixed point for a pair of oscillators coupled with only synaptic coupling. The function H_{gap} favors the in-phase state

for pairwise interactions so that 0 is a stable fixed point for a pair of oscillators coupled with only gap junction coupling. This is equivalent to saying that

A1. $H'_{syn}(0) < 0$

A2. $H'_{gap}(0) > 0$

For simplicity, we also need the following:

A3. $H_{syn}(0) = 0$

A4. $H_{gap}(0) = 0$

Note that, A4 holds automatically for gap junctions since a cell cannot be coupled to itself via gap junctions. If $H_{syn}(0) = \kappa \neq 0$, then let $\theta_j = \hat{\theta}_j + \Omega t$ where $\Omega = \omega + g_{syn}\kappa$. We write

$$\frac{d\hat{\theta}_j}{dt} = \frac{g_{syn}}{N}\sum_{k=1}^{N} \hat{H}_{syn}(\hat{\theta}_k - \hat{\theta}_j) + g_{gap}\sum_{\ell=-m}^{m} J_\ell H_{gap}(\hat{\theta}_{j+\ell} - \hat{\theta}_j), \quad \text{j=1,}\ldots,N$$

where $\hat{H}_{syn}(\phi) = H_{syn}(\phi) - \kappa$. We can see that, $\hat{H}_{syn}(0) = 0$, so w.l.o.g, we assume $H_{syn}(0) = 0$.

We also make a normalization assumption on J_ℓ by taking

A5*. $\sum_{l=-m}^{m} J_\ell = 1$

For the purposes of calculations, it is much easier to work with the continuum analogue of equation (2.3), so our analysis will be on a continuum version of the network. We also arrange the oscillators on a ring (instead of an array) to avoid boundary effects. Without loss of generality we assume the array was of length 2π and when wrapped around a ring

$x = 0$ and $x = 2\pi$ represents the same point. Hence, from now on, we study this model

$$\begin{aligned} \frac{\partial \theta}{\partial t} &= \omega + \frac{g_{syn}}{2\pi} \int_0^{2\pi} H_{syn}(\theta(y) - \theta(x))\ dy \\ &\quad + g_{gap} \int_0^{2\pi} J(x-y)\ H_{gap}(\theta(y) - \theta(x))\ dy \end{aligned} \tag{2.4}$$

where analogous assumptions are made as to the discrete model. We remark that the continuum model can be derived from the discrete model in the limit as $N \to \infty$ with suitable a normalization assumption on the function J_ℓ. One difference is in the discrete model, θ_j was a function of time and the discrete index, j, whereas it is now a function of time and space. We assume $J(x)$ is a non-negative, symmetric kernel around 0 and the normalization condition is

A5. $\int_0^{2\pi} J(y)\ dy = 1$.

In our numerical simulations, we used a truncated version of $J(x) = \sum_{n=-\infty}^{\infty} \exp(-(x + 2\pi n)^2)/\sqrt{\pi}$ (see Figure 2.3.2).

2.4 LINEAR STABILITY ANALYSIS FOR SYNCHRONOUS SOLUTION

We want to study the spatial interactions between synchronizing and anti-synchronizing influences. We start with the synchronous state and study its stability. The synchronous state is where all of the oscillators have the same phase. Note that if we assume heterogeneity in the intrinsic frequencies, synchrony is not a solution to the system. If we have homogeneity, $\theta(x,t) = \Omega t$ is a solution to (2.4) where $\Omega = \omega + g_{syn} H_{syn}(0)$ represents the frequency of the

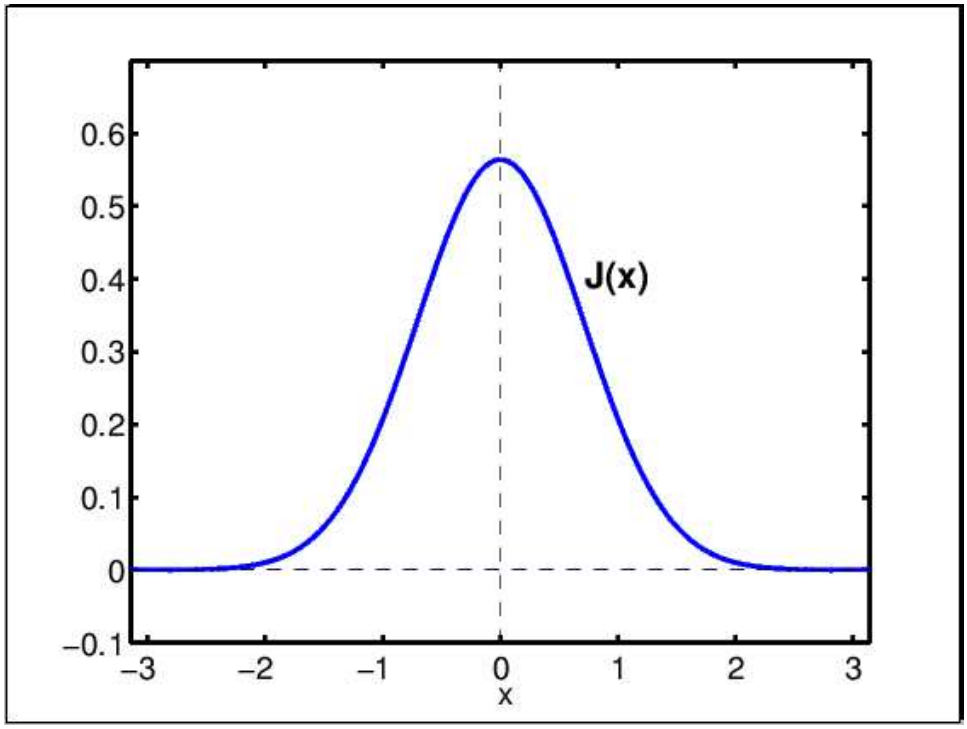

Figure 2.3.2: A plot of $J(x)$ where the sum was taken over $n = -2, -1, 0, 1, 2$.

network. To determine the stability of synchrony, we let $\theta(x,t) = \Omega t + \psi(x,t)$ and write

$$\begin{aligned} \frac{\partial \psi}{\partial t} &= \frac{g_{syn}}{2\pi} \int_0^{2\pi} H'_{syn}(0)\ [\psi(y) - \psi(x)]\ dy \\ &\quad + g_{gap} \int_0^{2\pi} J(x-y)\ H'_{gap}(0)\ [\psi(y) - \psi(x)]\ dy + O\left(|\psi|^2\right) \end{aligned} \tag{2.5}$$

If we only keep the linear terms above, we can see that $\psi(x,t) = e^{inx}\ e^{\lambda_n t}$ solves (2.5) with the appropriate choice of λ_n. Let $I_n = \int_0^{2\pi} J(s)\ e^{-ins}\ ds$, and substitute $\psi(x,t)$ into (2.5) to get

$$\lambda_n = -g_{syn}\ H'_{syn}(0) + g_{gap}\ H'_{gap}(0)\ [I_n - 1] \tag{2.6}$$

for $n \neq 0$. For $n = 0$, $\lambda_0 = 0$. We choose $J(x)$ so that we have $I_1 \geq 1$ and $I_1 > I_2 > \cdots > I_n > I_{n+1} > \ldots$. This means that the first Fourier mode dominates. The Gaussian kernel shown in Figure 2.3.2 satisfies this criterion as does, for example, the periodic version of an exponential kernel, $\exp(-|x|)$. With this assumption, it is easy to see that the first eigenvalue to cross over to positive values would be λ_1. We call $n = 1$ *the most unstable mode*. To find the critical value of g_{syn}, we solve for $\lambda_1 = 0$ which gives us

$$g^*_{syn} = \frac{g_{gap}\ H'_{gap}(0)\ [I_1 - 1]}{H'_{syn}(0)} \tag{2.7}$$

Here * is used to denote the value of g_{syn} at the bifurcation point. To study the stability of the bifurcating solutions we need to find the normal form for the bifurcation. We prove the following theorem.

Theorem 1 *The system (2.4) with the assumptions A1-A5 has a pitchfork bifurcation at* g^*_{syn} *and the corresponding normal form is:*

$$0 = \zeta z^2 \bar{z} + \eta z$$

The coefficients ζ *and* η *are:*

$$\begin{aligned} \zeta &= 12B_{1,3} - 3B_{2,3} - 9B_{0,3} + 2C\ B_{0,2} - 2CB_{2,2} \\ \eta &= -g_2\alpha_1 \end{aligned}$$

where

$$\begin{aligned} B_{n,j} &= \int_0^{2\pi} A_j(y')\ e^{iny'}\ dy' \\ A_j(x) &= \frac{g^*_{syn}}{2\pi}\ \alpha_j + g_{gap}\ \beta_j\ J(x) \\ C &= \frac{2B_{1,2} - B_{2,2} - B_{0,2}}{B_{2,1} - B_{0,1}} \end{aligned}$$

with $\alpha_j = \frac{H^j_{syn}(0)}{j!}$ *and* $\beta_j = \frac{H^j_{gap}(0)}{j!}$ *for* $j = 1, 2, \ldots$. *Here* $f^j(x_0)$ *represents the* i*th derivative at* x_0 *for* $f = H_{syn}, H_{gap}$ *and* g_2 *appears in the perturbation expansion for* g_{syn}.

Proof: We use a perturbation expansion for the solution ψ and g_{syn} as

$$\theta(x,t) = \Omega(\epsilon)\ t + \hat{\psi}(x,\epsilon) \tag{2.8}$$

where

$$\Omega(\epsilon) = \Omega + \epsilon\ \Omega_1 + \epsilon^2\ \Omega_2 + \epsilon^3\ \Omega_3 + \ldots \tag{2.9}$$

$$\hat{\psi}(x,\epsilon) = \epsilon\ \psi_1(x) + \epsilon^2\ \psi_2(x) + \epsilon^3\ \psi_3(x) + \ldots \tag{2.10}$$

and

$$g_{syn} = g^*_{syn} + \epsilon\ g_1 + \epsilon^2\ g_2$$

We define a linear operator $\mathcal{L}$ as follows

$$\begin{aligned}
\mathcal{L}\hat{\psi} &= \frac{g^*_{syn}}{2\pi}\int_0^{2\pi} H'_{syn}(0)[\hat{\psi}(y,\epsilon) - \hat{\psi}(x,\epsilon)]dy \\
&\quad + g_{gap}\int_0^{2\pi} J(x-y)H'_{gap}(0)[\hat{\psi}(y,\epsilon) - \hat{\psi}(x,\epsilon)]dy \\
&= \frac{g^*_{syn}}{2\pi}\int_0^{2\pi} H'_{syn}(0)[\hat{\psi}(x-y',\epsilon) - \hat{\psi}(x,\epsilon)]dy' \\
&\quad + g_{gap}\int_0^{2\pi} J(y')H'_{gap}(0)[\hat{\psi}(x-y',\epsilon) - \hat{\psi}(x,\epsilon)]dy' \qquad (2.11)
\end{aligned}$$

with the substitution $y' = x - y$. It is easy to notice that $e^{\pm ix}$, $\mathbf{1}$ are in the null space of $\mathcal{L}$ and $\mathcal{L}$ is self-adjoint (here and in Appendix B, we use $\mathbf{1}$ to denote the constant function which is 1 for all x). We need to find the Taylor expansions of H_{syn} and H_{gap} around 0 for the full system

$$\begin{aligned}
H_{syn}(x) &= H_{syn}(0) + H'_{syn}(0)\ x + \frac{H''_{syn}(0)}{2}\ x^2 + \frac{H'''_{syn}(0)}{6}\ x^3 + \ldots \\
&= \alpha_1\ x + \alpha_2\ x^2 + \alpha_3\ x^3 + \ldots
\end{aligned}$$

$$\begin{aligned}
H_{gap}(x) &= H_{gap}(0) + H'_{gap}(0)\ x + \frac{H''_{gap}(0)}{2}\ x^2 + \frac{H'''_{gap}(0)}{6}\ x^3 + \ldots \\
&= \beta_1\ x + \beta_2\ x^2 + \beta_3\ x^3 + \ldots
\end{aligned}$$

Substitute θ in the form given in (2.8) into (2.4)

$$\begin{aligned}
\Omega(\epsilon) &= \frac{(g^*_{syn}+\epsilon g_1+\epsilon^2 g_2)}{2\pi}\int_0^{2\pi}\alpha_1\,[\hat{\psi}(x-y',\epsilon)-\hat{\psi}(x,\epsilon)]\,dy' \\
&+\frac{(g^*_{syn}+\epsilon g_1+\epsilon^2 g_2)}{2\pi}\int_0^{2\pi}\alpha_2\,[\hat{\psi}(x-y',\epsilon)-\hat{\psi}(x,\epsilon)]^2\,dy' \\
&+\frac{(g^*_{syn}+\epsilon g_1+\epsilon^2 g_2)}{2\pi}\int_0^{2\pi}\alpha_3\,[\hat{\psi}(x-y',\epsilon)-\hat{\psi}(x,\epsilon)]^3\,dy' \\
&+g_{gap}\int_0^{2\pi}J(y')\,\beta_1\,[\hat{\psi}(x-y',\epsilon)-\hat{\psi}(x,\epsilon)]\,dy' \\
&+g_{gap}\int_0^{2\pi}J(y')\,\beta_2\,[\hat{\psi}(x-y',\epsilon)-\hat{\psi}(x,\epsilon)]^2\,dy' \\
&+g_{gap}\int_0^{2\pi}J(y')\,\beta_3\,[\hat{\psi}(x-y',\epsilon)-\hat{\psi}(x,\epsilon)]^3\,dy'+O\left(|\hat{\psi}|^4\right) \qquad (2.12)
\end{aligned}$$

Let $A_j(x)=\frac{g^*_{syn}}{2\pi}\,\alpha_j+g_{gap}\,\beta_j\,J(x)$ for $j=1,2,3$ and $Q(x)=\int_0^{2\pi}[\alpha_1(\hat{\psi}(x-y',\epsilon)-\hat{\psi}(x,\epsilon))+\alpha_2(\hat{\psi}(x-y',\epsilon)-\hat{\psi}(x,\epsilon))^2+\alpha_3(\hat{\psi}(x-y',\epsilon)-\hat{\psi}(x,\epsilon))^3]\,dy'$ which lets us to rewrite (2.12) as

$$\begin{aligned}
\Omega(\epsilon) &= \int_0^{2\pi}A_1(y')\,[\hat{\psi}(x-y',\epsilon)-\hat{\psi}(x,\epsilon)]\,dy' \\
&+\int_0^{2\pi}A_2(y')\,[\hat{\psi}(x-y',\epsilon)-\hat{\psi}(x,\epsilon)]^2\,dy' \\
&+\int_0^{2\pi}A_3(y')\,[\hat{\psi}(x-y',\epsilon)-\hat{\psi}(x,\epsilon)]^3\,dy' \\
&+\epsilon\,\frac{g_1}{2\pi}\,Q(x)+\epsilon^2\,\frac{g_2}{2\pi}\,Q(x)+O\left(|\hat{\psi}|^4\right) \qquad (2.13)
\end{aligned}$$

We match the coefficients of powers of ϵ terms from both sides of the equation (2.13). This allows us to compute the coefficients for the normal form. The rest of the calculations are given in Appendix B. The normal form for the bifurcation is:

$$0 = \zeta z^2\bar{z}+\eta z$$

where $\zeta = 12B_{1,3} - 3B_{2,3} - 9B_{0,3} + 2CB_{0,2} - 2CB_{2,2} - 2CB_{2,2}$ and $\eta = -g_2\alpha_1$. Note that η is positive since $\alpha_1 < 0$ from our assumptions. So, depending on the sign of ζ, we can determine the stability of the new solutions.

In our case, we compute $\zeta = -210.09$ and $\eta = 105g_2$ which tells us that we have a supercritical pitchfork bifurcation. Thus, the new solution bifurcating from synchrony is stable.

2.5 EXISTENCE AND STABILITY OF THE TRAVELING WAVE

Next, we look at the existence and stability of the traveling wave, $\theta(x,t) = \Omega t + x$. Substituting θ back into (2.4) gives us

$$\Omega = \omega + \frac{g_{syn}}{2\pi}\int_0^{2\pi} H_{syn}(y)dy + g_{gap}\int_0^{2\pi} J(y)H_{gap}(y)dy \tag{2.14}$$

Without loss of generality, we can assume that the average of H_{syn} is zero and let $I = \int_0^{2\pi} J(y)H_{gap}(y)dy$. Equation (2.14) reduces to $\Omega = \omega + g_{gap}I$. Note that the value of the frequency is irrelevant to the stability calculation since the right hand sides always involve terms of the form $\theta(x,t) - \theta(y,t)$ so that adding Ct to θ where C is any constant, has no effect. We prove the following theorem about the stability of the traveling wave.

Theorem 2 *The traveling wave solution, $\theta(x,t) = \Omega t + x$, is a stable solution to 2.4 if we have*

$$
\begin{aligned}
Re(\lambda_n) &= -\frac{1}{2}g_{syn}nb_n + 2\pi g_{gap}\sum_{m=-\infty}^{-n-1}\frac{m}{4}[(c_m f_{n+m} - d_m e_{n+m}) - (c_m f_m - d_m e_m)] \\
&\quad -2\pi g_{gap}\sum_{m=-n}^{-1}\frac{m}{4}[(c_m f_{n+m} + d_m e_{n+m}) + (c_m f_m - d_m e_m)] \\
&\quad -2\pi g_{gap}\sum_{m=1}^{\infty}\frac{m}{4}[(c_m f_{n+m} - d_m e_{n+m}) - (c_m f_m - d_m e_m)] \\
&\leq 0
\end{aligned}
$$

for $n > 0$ where

$$
\begin{aligned}
H_{syn}(y) &= \sum_{n=0}^{\infty} a_n \cos ny + b_n \sin ny \\
H_{gap}(y) &= \sum_{n=0}^{\infty} c_n \cos ny + d_n \sin ny \\
J(y) &= \sum_{n=0}^{\infty} e_n \cos ny + f_n \sin ny
\end{aligned}
$$

Proof: Letting $\theta(x,t) = \Omega t + x + \psi(x,t)$, we write

$$
\begin{aligned}
\frac{\partial \psi}{\partial t} &= \frac{g_{syn}}{2\pi}\int_0^{2\pi} H'_{syn}(y)\ [\psi(x+y) - \psi(x)]\ dy \\
&\quad + g_{gap}\int_0^{2\pi} J(-y)\ H'_{gap}(y)\ [\psi(x+y) - \psi(x)]\ dy + O\left(|\psi|^2\right)
\end{aligned} \tag{2.15}
$$

$\psi(x,t) = e^{inx}e^{\lambda_n t}$ solves (2.15) up to linear order. We solve for λ_n to get

$$
\lambda_n = \frac{g_{syn}}{2\pi}\int_0^{2\pi} H'_{syn}(y)[e^{iny} - 1]dy + g_{gap}\int_0^{2\pi} J(-y)\ H'_{gap}(y)[e^{iny} - 1]dy \tag{2.16}
$$

We look at the real part of λ_n, for H_{syn}, H_{gap} and J real-valued,

$$
Re(\lambda_n) = \frac{g_{syn}}{2\pi}\int_0^{2\pi} H'_{syn}(y)[\cos ny - 1]dy + g_{gap}\int_0^{2\pi} J(-y)\ H'_{gap}(y)[\cos ny - 1]dy
$$

When $n = 0$, $\lambda_0 = 0$ which corresponds to translation invariance. We need $Re(\lambda_n) \leq 0$ for $n \neq 0$. Also, we want to make our analysis as general as possible. For this reason we use the complex Fourier series expansion for H_{syn}, H_{gap} and J. Let $J(y) = \sum_{k=-\infty}^{\infty} \alpha_k e^{iky}$, $H_{syn}(y) = \sum_{l=-\infty}^{\infty} \beta_l e^{ily}$, $H_{gap}(y) = \sum_{m=-\infty}^{\infty} \gamma_m e^{imy}$ where $\alpha_{-k} = \alpha_k$, $\beta_{-l} = \beta_l$ and $\gamma_{-m} = \gamma_m$. Substituting these in 2.16 gives

$$\lambda_n = -ig_{syn} n\beta_{-n} + 2\pi i g_{gap} \sum_{m=-\infty}^{\infty} [m\gamma_m(\alpha_{-(n+m)} - \alpha_{-m})]$$

If we look at the real part of λ_n, we see that

$$\begin{aligned} Re(\lambda_n) &= -\frac{1}{2} g_{syn} n b_n + 2\pi g_{gap} \sum_{m=-\infty}^{-n-1} \frac{m}{4}[(c_m f_{n+m} - d_m e_{n+m}) - (c_m f_m - d_m e_m)] \\ &\quad -2\pi g_{gap} \sum_{m=-n}^{-1} \frac{m}{4}[(c_m f_{n+m} + d_m e_{n+m}) + (c_m f_m - d_m e_m)] \\ &\quad -2\pi g_{gap} \sum_{m=1}^{\infty} \frac{m}{4}[(c_m f_{n+m} - d_m e_{n+m}) - (c_m f_m - d_m e_m)] \end{aligned} \tag{2.17}$$

where H_{syn}, H_{gap}, and J are given with the Fourier expansion with coefficients $a_0 = 2\beta_0$, $c_0 = 2\gamma_0$, $e_0 = 2\alpha_0$, $a_n = \beta_n + \beta_{-n}$, $b_n = i(\beta_n - \beta_{-n})$, $c_n = \gamma_n + \gamma_{-n}$, $d_n = i(\gamma_n - \gamma_{-n})$, $e_n = \alpha_n + \alpha_{-n}$ and $e_n = i(\alpha_n - \alpha_{-n})$.

In our case, the traveling wave is always stable. Substituting into 2.17, we see that $Re(\lambda_n) \leq -50 g_{syn} - 824.27 g_{gap} \leq 0$ for all positive values of g_{syn}, and g_{gap}. We also note that a traveling wave in the opposite direction, $\theta(x,t) = \Omega t - x$ is also a solution to (2.14).

We close this section with some comments on the existence and stability of traveling waves in the discrete system for local gap junction coupling. Consider a discrete ring:

$$\frac{d\theta_j}{dt} = \omega + \sum_{i=-m}^{m} a_i H(\theta_{j+m} - \theta_j)$$

where $m \ll N$ and N is the number of oscillators. The coupling constants a_i are non-negative. Suppose that H is $2\pi-$periodic and $H'(x) > 0$ for $-r < x < r$ and $r > 0$. Then, it follows from [19] that the synchronous state is asymptotically stable. Now, consider a traveling wave:

$$\theta_j = \Omega t + 2\pi j/N.$$

This satisfies the discrete model if and only if

$$\Omega = \omega + \sum_{i=-m}^{m} a_i H(2\pi i/N).$$

If m/N is sufficiently small, then

$$H'(\pm 2\pi m/M) > 0$$

since $H'(x)$ is positive in some neighborhood of 0. Thus, again from [19] the traveling wave is asymptotically stable. Figure 2.3.1b shows that $H'_{gap}(x) > 0$ over more than half the cycle surrounding the origin. Thus, we can pick m as large as $N/4$ and still be assured that the traveling wave is stable. This shows that there is bistability between traveling waves and synchrony in the discrete model with small enough synaptic coupling.

2.6 NUMERICAL RESULTS

In this section we (i) show that the bifurcation theory developed for the continuum model appears to hold for the discrete model by numerically simulating the latter, (ii) numerically extend the local bifurcation analysis to get the full picture for the discrete phase-model, (iii) numerically simulate the conductance-based model and show similar patterns as found via

our analysis, and (iv) compute the bifurcation diagram for a line of 20 oscillators which are *not* connected in a ring.

Figure 2.6.1 depicts the steady-state relative phases for a ring of 20 phase-oscillators using the interaction functions shown in figure 2.3.1. The strength of the gap junction coupling is fixed as $g_{gap} = 1$ and g_{syn} is varied along the vertical axis. Simulations are done by starting the relative phases close to synchrony and then letting them evolve until a steady state is reached. Figure 2.6.1(a) shows this steady state (color-coded) for each value of g_{syn} examined. We remark that in the phase model, the absolute values of the coupling parameters is irrelevant and only their ratio matters. Figure 2.6.1(b) shows vertical cross sections from part (a) to more clearly illustrate different types of solutions observed for various g_{syn} values. For example, when $g_{syn} = 0.3$, there is no difference in phases of the oscillators indicating that the system is synchronized. In contrast, between $g_{syn} \approx 0.35$ and $g_{syn} \approx 0.87$, the solution is the patterned state which bifurcates from the synchronous state as described in section 3. As ρ increases beyond 0.87, the patterned state (which qualitatively resembles a cosine wave) disappears and leaves a traveling wave as the only solution. The traveling wave is, in fact, stable for all values of g_{syn} shown in the diagram so that for $g_{syn} < 0.87$, there is bistability. The loss of stability of the synchronous state occurs at $g_{syn} \approx 0.35$ which is very close to the value predicted in section 2 of 0.3476.

To give the reader some intuition for the patterns, we depict the spatio-temporal patterns in terms of their absolute phase in Figure 2.6.2. As we increase the relative coupling strength, we see the transition from synchrony to a stable patterned state (compare 2.6.2(a) to (b)). This is the state which arises via the pitchfork bifurcation calculated in section 2. As we further increase g_{syn}, the patterned state disappears and produces traveling waves; the

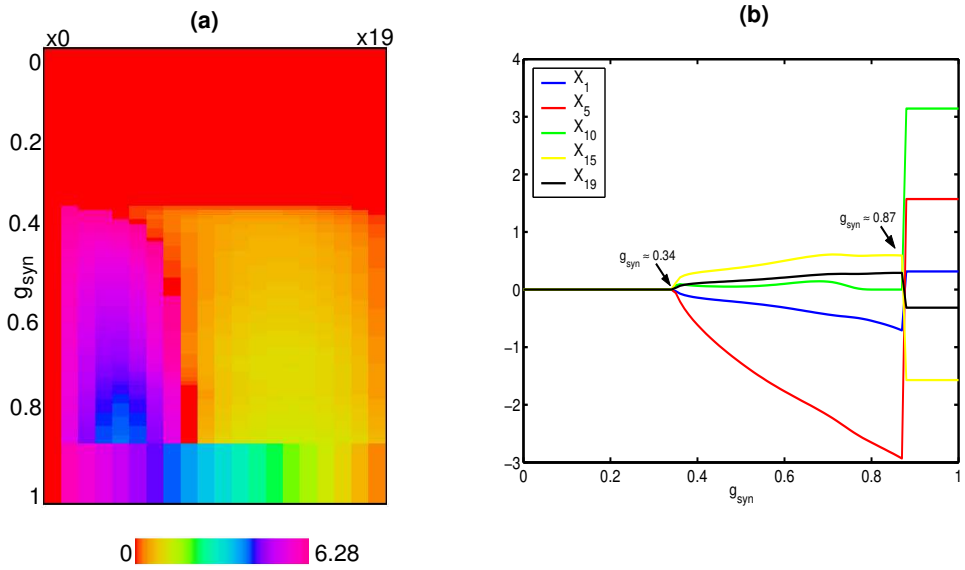

Figure 2.6.1: Transition from synchrony to intermediate state and then to traveling wave.

(a) illustrates an array plot of the relative phases of the oscillators as g_{syn} is increased and $g_{gap} = 1$. For small amounts of synaptic coupling, synchrony is stable. Around $g_{syn} = 0.35$, synchrony loses stability and a stable sinusoidal pattern emerges. This pattern also becomes unstable around $g_{syn} = 0.87$. There is a stable traveling wave solution for all the values of the parameter g_{syn} for any fixed value of g_{gap}. The system has bistability between the traveling wave and synchrony and the traveling wave and the intermediate state.

(b) displays vertical cross sections from the left panel as g_{syn} is increased and $g_{gap} = 1$. The bifurcation from synchrony and the intermediate state can be seen in more detail here.

transition from the patterned state to the waves is shown in figure 2.6.2(c). Finally, for larger g_{syn}, only the traveling wave remains.

The analytic calculations along with the numerical calculations of the phase reduced model show that as the inhibition increases, the synchronous state loses stability to a patterned state in which the relative phases are close to a cosine wave. Further increases in the inhibition result in a deepening of this pattern followed by a transition to a traveling wave. In figure 2.6.3, we show the result of a simulation of the biophysical model as the synaptic inhibition increases. To match the theory, we have made the connections periodic so that the last cell is coupled to the first. Figure 2.6.3(a) shows a clear phase pattern in which the oscillators at the end lag the ones in the middle. This corresponds to the patterned state shown in figure 2.6.2(b) and figure 2.6.1(a), when $g_{syn}/g_{gap} \approx 0.4$. For a larger amount of inhibition, the behavior becomes quite complicated and after a long transient begins a transition to traveling waves as shown in figure 2.6.3(b). Thus, the phase model provides a very good description of the full biophysical model and has the advantage of being simple enough to analyze.

We conclude this section with some comments on the simplification to a ring of oscillators instead of a line as in the original model. The main reason for assuming a ring is that the analytic calculations are then possible. If, instead of a ring, we consider a line of oscillators and choose the coupling functions so that the synchronous state exists, we can explore the stability and bifurcations as the anti-synchronous (synaptic inhibition) coupling increases. Rather than attempt these calculations analytically, we instead display numerical simulations for the phase model with all-to-all synaptic coupling and nearest neighbor gap junction coupling. Figure 2.6.4 shows the behavior for a line of 20 oscillators. By considering a linear

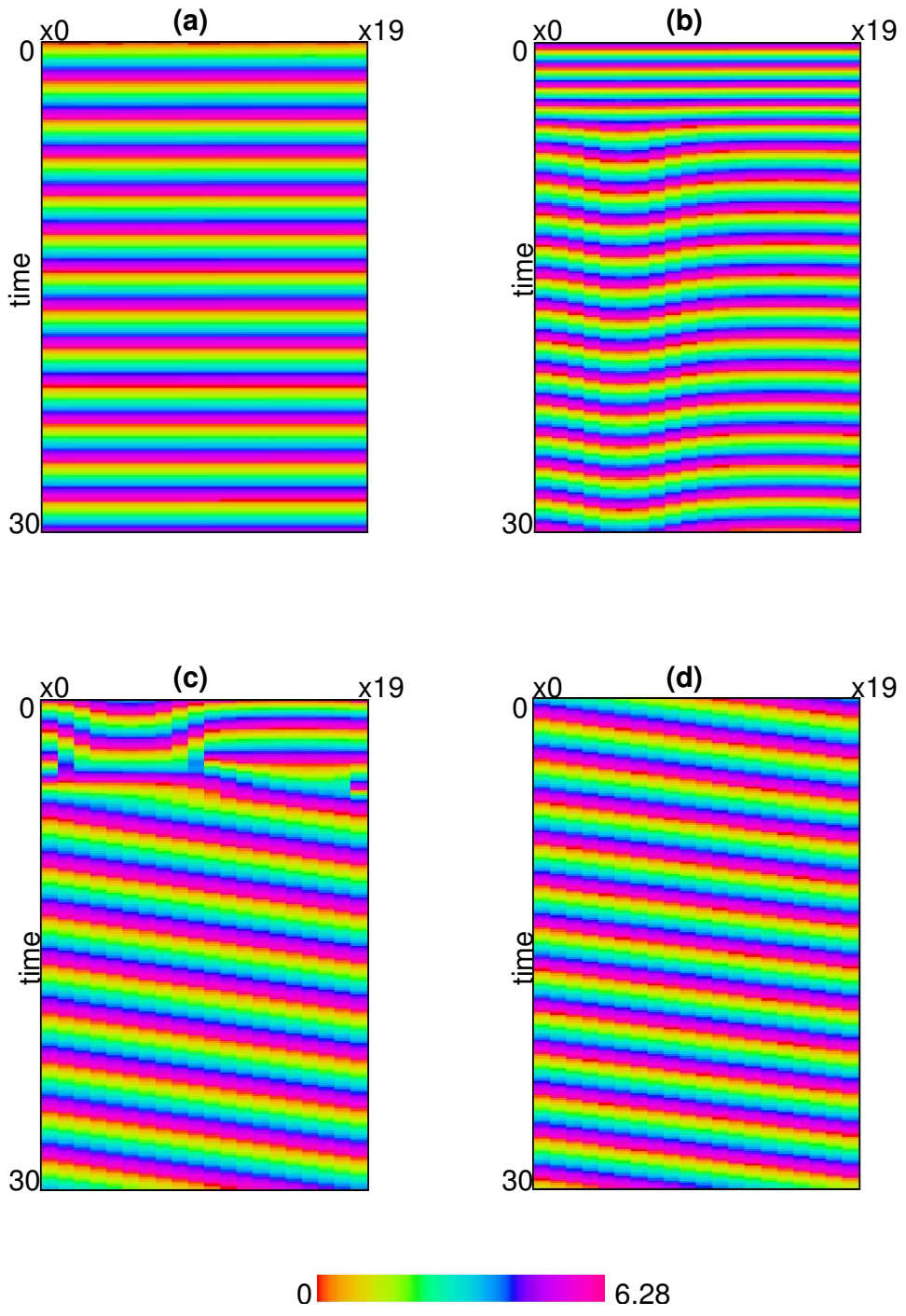

Figure 2.6.2: Evolution of the solution to the discrete phase model is shown as we change g_{syn} while g_{gap} is kept at the value 0.03. (a) shows synchronous solution when $g_{syn} = 0.01$, (b) shows the intermediate state when $g_{syn} = 0.02$, (c) shows the transition to the traveling wave solution when $g_{syn} = 0.03$, and (d) shows the traveling wave solution when $g_{syn} = 0.04$.

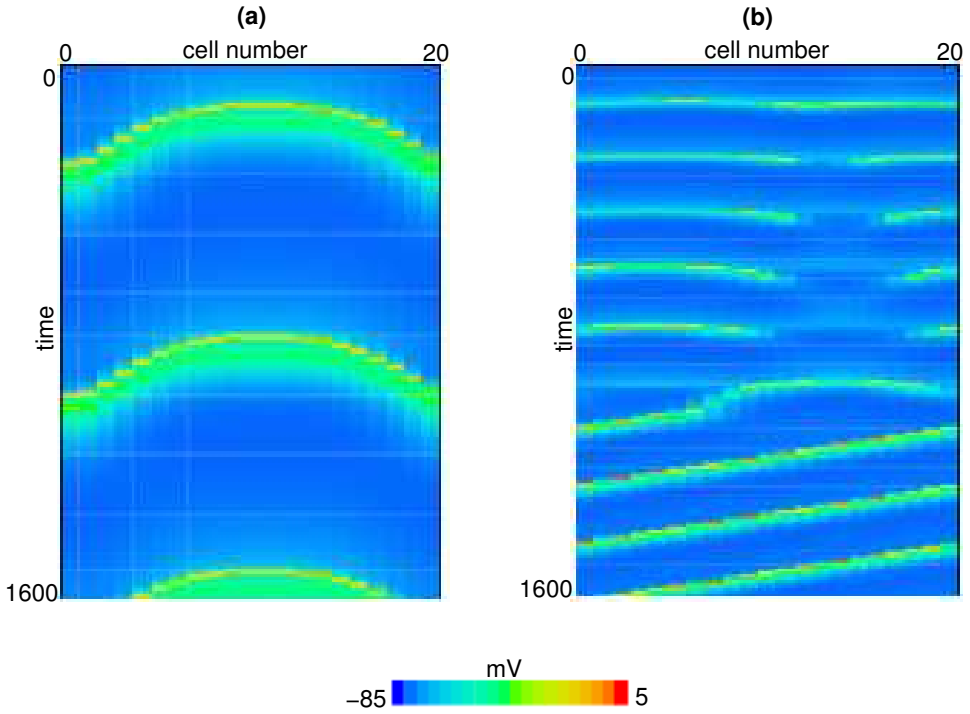

Figure 2.6.3: Behavior of the conductance-based model for $g_{syn} = 0.03$ and $g_{syn} = 0.07$. Voltage is plotted for each oscillator.

array, the symmetry in the ring model was broken and we are able to use AUTO bifurcation package [12]. We depict two pitchfork bifurcations. The first emerges as a stable supercritical bifurcation. The pattern is like a half of a cosine wave as opposed to the full cycle seen in a ring. The ring of oscillators can be imagined as a pair of lines joined symmetrically through the midline. Thus, we expect that the first bifurcation would be "half" of that seen in the ring (See curve 1 in Figure 2.6.4(b)). As g_{syn} increases, this branch seems to approach a solution which looks like a traveling wave (Figure 2.6.4(b) curves 2,3). There is no true traveling wave in the line due to the boundary conditions, however, the solutions in the figure look like traveling waves. A second branch bifurcates supercritically but it inherits the instability of the synchronous branch, so that it is unstable. The shape of this solution is shown by curve 4 in Figure 2.6.4(b). As these solutions were unstable, they were not continued beyond $g_{syn} = 0.5$. Thus, while the details are somewhat different, the ultimate result is the same for both a ring and a linear array: as g_{syn} increases, synchrony loses stability and for large enough g_{syn} there is a traveling wave. The traveling wave exists for all values of g_{syn} in the ring model but not for the linear array.

2.7 CONCLUSIONS

In this chapter, we have shown that the combination of long range inhibitory synaptic coupling with local gap junction coupling was sufficient to induce a destabilization of the synchronous state. A new state which is not a traveling wave, but rather, a spatially organized phase shift stably appears and is lost as the amount of long range inhibitory coupling increases. Numerical solutions indicate that the only remaining attracting state is a traveling

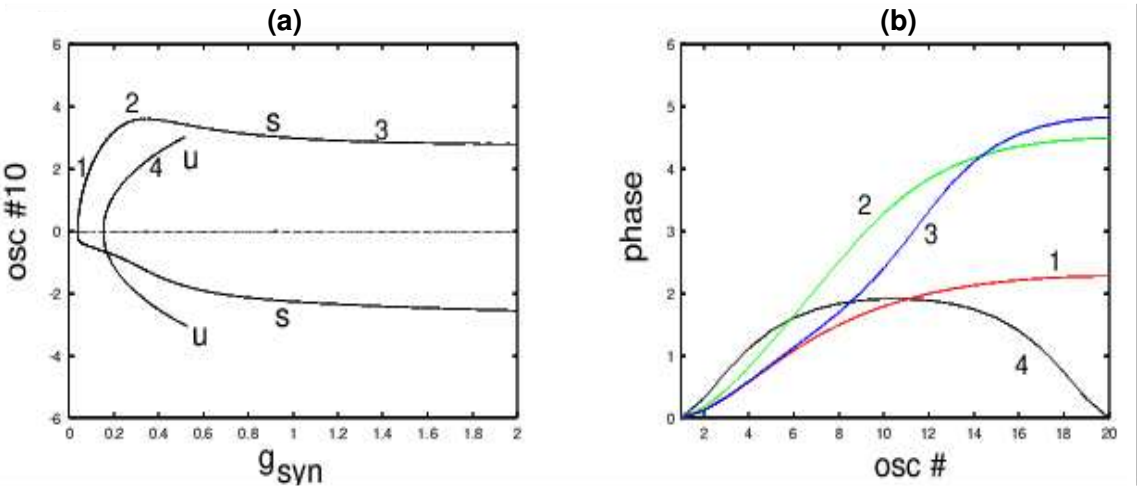

Figure 2.6.4: Behavior of 20 phase oscillators in a *line* as the synaptic coupling increases.(a) The relative phase of oscillator 10; $g_{gap} = 1$ and the interaction functions are same as in the ring model, (b) Spatial profiles with various solutions from (a). u refers to the solution being unstable and s means the solution is stable.

wave. Our mathematical results concern a network on a ring; the original motivation for this problem is the slug olfactory lobe which is actually a line of oscillators. However, it is known from earlier work [41] that boundary effects are enough to induce patterns of phases which depend very strongly on the choices of boundary conditions at the edges. To avoid this difficulty, we have considered periodic boundary conditions which eliminate questions about the behavior at the edges. In spite of this simplifying assumption, we see that the linear array and the ring behave similarly at least when the inhibition is sufficiently large compared to electrical coupling.

A number of studies have investigated interactions between electrical coupling and synaptic coupling between neural oscillators. This problem is important since inhibitory interneurons in the mammalian neocortex appear to be coupled with both types of interactions. These networks may act as the "pacemakers" for 40 Hz oscillations observed the cortex during various cognitive tasks [57]. Most theoretical explorations involve either pairs of cells or globally coupled networks. In most instances, both the synaptic and the electrical coupling encourage synchrony so that there is not a chance for pattern formation. However, [8] has shown that gap junctions can either stabilize or destabilize synchrony depending on the shape of the action potential while [49] have shown that the intrinsic currents also affect whether or not electrical coupling is synchronizing. Combining coupling which destabilizes with coupling that stabilizes synchrony can be expected to produce other patterns of activity besides waves. Such patterns may play some role in cortical processing of information and may confer certain computational advantages [14].

3.0 CLUSTERING IN COUPLED NEURAL OSCILLATORS

3.1 INTRODUCTION

Globally coupled oscillators have been studied extensively [2, 7, 51, 52, 53] . Such systems arise in natural and physical environments such as flashing fireflies, chirping crickets, multi-mode lasers and networks of oscillatory neurons. The analysis is simple enough in the case of mean-field coupling where the interactions among oscillators is represented by an average or effective interaction. In such a system, there is a lack of spatial structure and one would expect that the types of activity patterns observed should also be simple. However, it has been shown that even in a network of identical oscillators with global coupling, it is possible to go from synchrony to clustered states and to asynchrony [3, 27, 31, 48]. In these papers, the network dynamics were explored by using simple sinusoidal coupling functions or by adding noise to the system.

In this chapter, we want to study a system of coupled ring oscillators with inhibitory all-to-all connections which exhibits a stable two-cluster state. We add spatial structure by nearest neighbor gap junctions. We still have a symmetric network since the oscillators are organized on a ring. Gap junction coupling has a synchronizing effect on the oscillators by itself.

In the following section, we describe the model with only all-to-all coupling and go through the stability analysis for the two-cluster state. The analysis is similar to the work done in [31]. They consider a network of synaptically coupled Hodgkin-Huxley neurons whose interactions are described using a phase model. They find n-cluster solutions with $n > 1$ where the network breaks up into n subgroups inside which the oscillators are phase-locked. For the choice of coupling function and model parameters, they observe pairs of unstable two cluster states that are connected by heteroclinic orbits.

In Section 3.3, we provide an extension to the model given in Section 3.2 by adding a small amount of gap junction coupling. We find a traveling wave solution which is stable for a wide range of values of the parameter g_{gap} and loses its stability at a Hopf bifurcation. There are other stable solutions possible for the system and we explore them as well.

In the fourth section we numerically simulate a network of oscillators and justify our analytical results from previous sections. We simulate networks with various sizes and look at the changing behavior. Our broad aim in this chapter is to show that even a simple network with electrical and chemical coupling can exhibit a large variety of activity patterns. Simplicity of the network architecture doesn't mean simplicity in the behavior we get from the network.

3.2 THE BASE MODEL

We start our analysis by recapping the work in [31]. Consider a globally coupled network of identical phase oscillators given by the equation

$$\frac{d\theta_j}{dt} = \omega \ + \frac{g_{syn}}{N} \sum_{k=1}^{N} H_{syn}(\theta_k - \theta_j) \quad \text{for} \quad j = 1, .., N \tag{3.1}$$

where θ_j represents the phase of oscillator j and ω is the intrinsic frequency of the network. Without coupling, each oscillator is moving around its limit cycle with frequency ω. The case where the oscillators have different frequencies has also been studied but we will not consider it in this section. H_{syn} is the function representing the inhibitory interactions between the oscillators for which g_{syn} is the strength of coupling. We will give details about the coupling functions once we establish the general results. We are interested in clustered solutions to (3.1). We look at the case where m of the oscillators have phase $\theta_A = \Omega t$ and the remaining $N - m$ have phase $\theta_B = \Omega t + \phi$ with $\phi \in [0, 2\pi]$. By letting $p = \frac{m}{N}$, we can rewrite (3.1) as

$$\begin{aligned} \theta_A^{'} &= \omega + g_{syn}(pH_{syn}(0) + (1-p)H_{syn}(\theta_B - \theta_A)) \\ \theta_B^{'} &= \omega + g_{syn}(pH_{syn}(\theta_A - \theta_B) + (1-p)H_{syn}(0)) \end{aligned}$$

which then becomes

$$\begin{aligned} \Omega &= \omega + g_{syn}(pH_{syn}(0) + (1-p)H_{syn}(\phi)) \\ \Omega &= \omega + g_{syn}((1-p)H_{syn}(0) + pH_{syn}(-\phi)) \end{aligned}$$

Subtracting the first equation from the second, we get

$$0 = g_{syn}((1-p)H_{syn}(0) + pH_{syn}(-\phi) - pH_{syn}(0) - (1-p)H_{syn}(\phi)) \tag{3.2}$$

Regrouping the terms in (3.2), we can solve for p

$$p = \frac{H_{syn}(0) - H_{syn}(\phi)}{2H_{syn}(0) - H_{syn}(-\phi) - H_{syn}(\phi)} \equiv F(\phi) \tag{3.3}$$

where $F(\pi) = 1/2$. Given H_{syn} and ϕ, we can determine the size of the clusters according to (3.3). So far, we have established the existence of two-cluster states. One could also look at other n-cluster states but we limit our analysis to two-cluster states and study the stability. We look at the linearization about the two-cluster state. Let $\theta_j = \Omega t + y_j$ where y_j are small perturbations, we get

$$\frac{dy_j}{dt} = \frac{g_{syn}}{N} \sum_{k=1}^{N} H'_{syn}(\theta_k - \theta_j)(y_k - y_j) \quad \text{for} \quad j = 1, ..N \tag{3.4}$$

which can be written as two separate equations

$$\begin{aligned} y_j' &= \frac{g_{syn}}{N} \sum_{k=1}^{m} H'_{syn}(0)(y_k - y_j) + \frac{g_{syn}}{N} \sum_{k=m+1}^{N} H'(\phi)(y_k - y_j) \quad \text{for} \quad j = 1, .., m \\ y_j' &= \frac{g_{syn}}{N} \sum_{k=1}^{m} H'(-\phi)(y_k - y_j) + \frac{1}{N} \sum_{k=m+1}^{N} H'(0)(y_k - y_j) \quad \text{for} \quad j = m+1, .., N \end{aligned}$$

Letting $\alpha = H'_{syn}(0)$, $\beta = H'_{syn}(\phi)$, $\gamma = H'_{syn}(-\phi)$, $\xi = -(m-1)\alpha - (N-m)\beta$, $\nu = -m\gamma - (N-m-1)\alpha$ and

$$A = \begin{bmatrix} \xi & \alpha & \cdots & \alpha \\ \alpha & \xi & \cdots & \alpha \\ \vdots & \vdots & \ddots & \vdots \\ \alpha & \cdots & \alpha & \xi \end{bmatrix},$$

$$B = \alpha \vec{\mathbf{1}}_{m\times(N-m)} \quad ,$$

$$C = \gamma \vec{\mathbf{1}}_{(N-m)\times m} \quad \text{and}$$

$$D = \begin{bmatrix} \eta & \alpha & \cdots & \alpha \\ \alpha & \eta & \cdots & \alpha \\ \vdots & \vdots & \ddots & \vdots \\ \alpha & \cdots & \alpha & \eta \end{bmatrix}$$

we can write (3.4) as:

$$\mathbf{y}' = g_{syn}\mathbf{M}\mathbf{y} \tag{3.5}$$

where $\mathbf{y} = \begin{bmatrix} y_1 & y_2 & \cdots & y_N \end{bmatrix}^T$ and $M = \frac{1}{N}\begin{bmatrix} A & B \\ C & D \end{bmatrix}$. In order to determine the stability of the two-cluster state, we need to find the eigenvalues of the matrix M. A similar analysis was done in [31]. We state the following theorem:

Theorem 3 *The eigenvalues of the matrix M in 3.5 are:*

$$\begin{aligned}
\lambda_1 &= -p\alpha - (1-p)\beta \\
\lambda_2 &= -p\gamma - (1-p)\alpha \\
\lambda_3 &= -p\gamma - (1-p)\beta \\
\lambda_4 &= 0
\end{aligned}$$

where $p = \frac{m}{N}$. The algebraic multiplicities of λ_1, λ_2, λ_3 and λ_4 are $m-1$, $N-m-1$, 1 and 1, respectively.

Proof: The original system has translation invariance, which means that if $\theta_j = \Omega t$ is a solution, then so is $\theta_j + \phi$. The zero eigenvalue, λ_4, corresponds to this property. The associated eigenvector is found as

$$v_4 = \begin{bmatrix} 1 & 1 & \cdots & 1 \end{bmatrix}^T.$$

λ_1, λ_2 are the eigenvalues that correspond to fluctuations within a cluster, whereas λ_3 corresponds to fluctuations between the two clusters. The associated eigenvector for λ_3 has the form

$$v_3 = \begin{bmatrix} 1 & \cdots & 1 & x & \cdots & x \end{bmatrix}^T$$

where $x \neq 1$. We need to solve the equation $Mv_3 = \lambda_3 v_3$ in order to get λ_3 and v_3.

$$Mv_3 = \begin{bmatrix} (x-1)(1-p)\beta x \\ \vdots \\ (x-1)(1-p)\beta x \\ -(x-1)p\gamma \\ \vdots \\ -(x-1)p\gamma \end{bmatrix} = \lambda_3 \begin{bmatrix} 1 \\ \vdots \\ 1 \\ x \\ \vdots \\ x \end{bmatrix}$$

which implies $(x-1)(1-p)\beta x = \lambda_3$ and $-(x-1)p\gamma = \lambda_3 x$. We solve for x to get $x = \frac{-p\gamma}{(1-p)\beta}$ and $\lambda_3 = -p\gamma - (1-p)\beta$.

We next claim that the eigenvector, v_1, associated with λ_1 has the form $\begin{bmatrix} \boldsymbol{\nu_1} \\ \mathbf{0} \end{bmatrix}$ where ν_1 is in the nullspace of C and $A\nu_1 = \lambda_1 \nu_1$. We write A as:

$$A = \begin{bmatrix} \xi & \alpha & \cdots & \alpha \\ \alpha & \xi & \cdots & \alpha \\ \vdots & \vdots & \ddots & \vdots \\ \alpha & \cdots & \alpha & \xi \end{bmatrix} = \begin{bmatrix} \xi-\alpha & 0 & \cdots & 0 \\ 0 & \xi-\alpha & \cdots & 0 \\ \vdots & \vdots & \ddots & \vdots \\ 0 & \cdots & 0 & \xi-\alpha \end{bmatrix} + \underbrace{\begin{bmatrix} \alpha & \cdots & \alpha \\ \vdots & \ddots & \vdots \\ \alpha & \cdots & \alpha \end{bmatrix}}_{\hat{A}}$$

If $\hat{\lambda} \in \sigma(\hat{A})$, then $\hat{\lambda} + \xi - \alpha \in \sigma(A)$. 0 is an $m-1$-fold eigenvalue for the matrix $\hat{A}$ which implies the eigenvalues of A are $\xi - \alpha$ with corresponding eigenvector ν_1. Substituting ξ back we get $\lambda_1 = -p\alpha - (1-p)\beta$. λ_2 can be found similarly.

An immediate corollary of Theorem (3) implies that the eigenvalues for the system given in (3.5) are 0, $g_{syn}\lambda_1$, $g_{syn}\lambda_2$, $g_{syn}\lambda_3$. For stability of the two-cluster solution, the real parts of the eigenvalues have to be negative. This translates into the following conditions for stability:

- $p\alpha + (1-p)\beta > 0$
- $p\gamma + (1-p)\alpha > 0$
- $p\gamma + (1-p)\beta > 0$

3.2.1 Application

In the previous chapter, we developed a phase model to explain the occurrence of traveling waves in the olfactory lobe of Limax. The oscillators were coupled through all-to-all inhibitory synaptic coupling and local electrical coupling via gap junctions. Here, we want to use the ideas and intuition from that paper and look at the contradicting effects of these two couplings on the system. To accommodate what we want to achieve, we use the coupling functions computed from the biophysical model in [13] with a slight modification. We only change the coefficient of $\sin(2x)$ from -5 to 5. The coupling functions are:

$$H_{syn}(x) = 35 + 200\cos(x) + 32\cos(2x) - 95\sin(x) + 5\sin(2x)$$

$$H_{gap}(x) = 87 - 50\cos(x) - 37\cos(2x) + 295\sin(x) - 65\sin(2x)$$

We remind the reader that the choice of coupling functions will determine what kind of solutions we get. Changing the coefficient of $\sin(2x)$ in this manner allows for the existence and stability of two-cluster states. Figure 3.2.1 represents the relation between p and ϕ. For values of ϕ ranging from 0 to 2π, we are able to find the size of each cluster using (3.3). From now on, we want to look at equal size clusters, so $p = 1/2$. In the case of different size clusters, the Implicit Function Theorem can be used to get stability conditions for the solutions. Substituting the value of p in (3.2) we get:

$$0 = \frac{g_{syn}}{2}[H_{syn}(-\phi) - H_{syn}(\phi)]$$

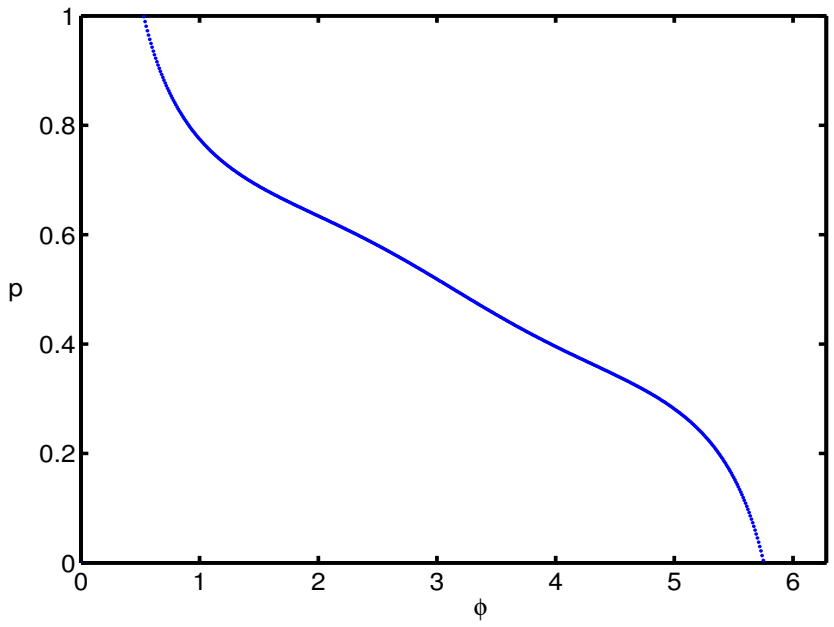

Figure 3.2.1: Possible values for p are graphed as the phase difference, ϕ varies from 0 to 2π

Let $g(x) = H_{syn}(-x) - H_{syn}(x)$. H_{syn} is a 2π-periodic function so, 0 and π are fixed points for g. For two oscillators, we need to have $H'_{syn}(0) > 0$ for the stability of the synchronous state and $H'_{syn}(\pi) > 0$ for the stability of the two-cluster state which corresponds to the anti-phase locked solution. The synchronous state was studied in **??**.

Next, we compute the eigenvalues for the linearized system in order to determine the stability of the two-cluster state with $(p, \phi) = (1/2, \pi)$. Figure 3.2.2 represents the values of the eigenvalues for each possible value for the pair (p, ϕ). As we can see from the figure, there is a small window of values of ϕ around π, where all the eigenvalues are negative. From our stability conditions we need to satisfy:

- $H'_{syn}(0) + H'_{syn}(\pi) > 0$,
- $H'_{syn}(0) + H'_{syn}(-\pi) > 0$ and
- $H'_{syn}(\pi) + H'_{syn}(-\pi) > 0$.

Since H_{syn} is 2π-periodic, we have $H'_{syn}(\pi) = H'_{syn}(-\pi)$. We also know that $H'_{syn}(0) < 0$ and the last stability condition can be rewritten as $H'_{syn}(\pi) > 0$. Thus, the stability condition in our case is:

- $H'_{syn}(0) + H'_{syn}(\pi) > 0$
- $H'_{syn}(\pi) > 0$
- $H'_{syn}(0) < 0$

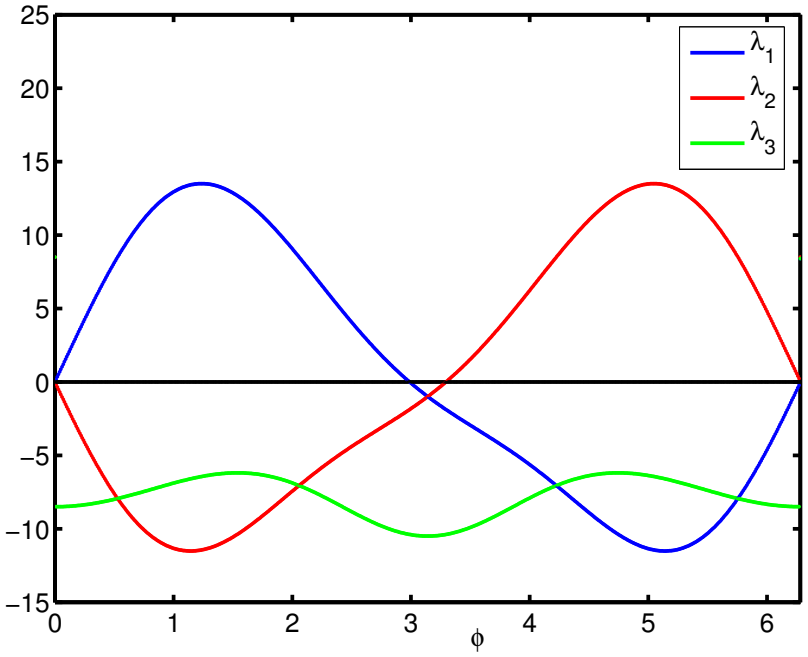

Figure 3.2.2: Eigenvalues for the system in 3.5 are computed for all possible values of (p, ϕ).

3.3 THE FULL MODEL WITH GAP JUNCTIONS

Once we have a system with stable two-cluster state solutions, we want to see what happens to these solutions as we add small amounts of nearest neighbor gap junction coupling. Equation (3.1) becomes

$$\frac{d\theta_j}{dt} = \frac{g_{syn}}{N}\sum_{k=1}^{N} H_{syn}(\theta_k - \theta_j) + g_{gap}[H_{gap}(\theta_{j+1} - \theta_j) + H_{gap}(\theta_{j-1} - \theta_j)] \tag{3.6}$$

where H_{gap} and g_{gap} represent the gap junction coupling function and its strength, respectively. H_{syn} by itself promotes asynchrony, whereas H_{gap} has synchronizing effects. The coupling functions are derived from the biophysical model given in [13], hence, H_{syn} represents the synaptic inhibition between bursting neurons.

In Chapter 2, we looked at a network where the scope of the gap junctions extended beyond the nearest neighbors. We found that in that case, a traveling wave was a stable solution for all the values of the parameters. We want to see if this holds here also. We start by noting that the traveling wave solution, $\theta_j = \Omega t + \frac{2\pi j}{N}$, satisfies (3.6) where

$$\Omega = \frac{g_{syn}}{N}\sum_{l=1}^{N} H_{syn}(\delta l) + g_{gap}(H_{gap}(\delta) + H_{gap}(\delta))$$

where $\delta = \frac{2\pi}{N}$. Given N, H_{syn}, H_{gap}, g_{syn} and g_{gap}, we can determine Ω uniquely up to sign. We want to study the stability of the traveling wave solution. In order to avoid edge effects, we assume the oscillators are arranged on a ring. The linearized system can be written as:

$$\frac{dy_j}{dt} = \frac{g_{syn}}{N}\sum_{l=1}^{N} H'_{syn}(\delta l)(y_{j+l} - y_j) + g_{gap}[H'_{gap}(\delta)(y_{j+1} - y_j) + H'_{gap}(-\delta)(y_{j-1} - y_j)] \tag{3.7}$$

The solutions for (3.7) are of the form $y_j = e^{\lambda_m t}e^{i\delta mj}$ where $j = 1, \ldots, N$, $m = 0, \ldots, N-1$. Solving for λ_m gives us:

$$\lambda_m = \frac{g_{syn}}{N}\sum_{l=1}^{N} H'_{syn}(\delta l)(e^{i\delta ml}-1) + g_{gap}[H'_{gap}(\delta)(e^{i\delta m}-1) + H'_{gap}(-\delta)(e^{-i\delta m}-1)]$$

To determine the stability, we look at the real parts of λ_m. For $m = 0$, we have $\lambda_0 = 0$ which corresponds to translation invariance. For $m \neq 0$, we need to use the Fourier series expansions of H'_{syn}, and H'_{gap}. Using the approximations for the coupling functions we see that $Re(\lambda_2)$ becomes 0 when $g_{gap} = 0.0746 g_{syn}$ for 20 oscillators. The imaginary part of λ_2 is nonzero which means there is a Hopf bifurcation at this point. Considering different size networks changes the value of g_{gap} where the Hopf bifurcation occurs. Figure 3.3.1 displays the values of critical coupling strength as N changes. For small networks, the traveling wave is stable for a wide range of parameters, whereas as the network size grows, it loses stability early on.

3.4 NUMERICAL RESULTS

In this section we numerically simulate a system of oscillators coupled with inhibition and nearest neighbor gap junctions. The oscillators are arranged on a ring to avoid boundary effects. Considering a linear array instead of the ring doesn't change the qualitative behavior of the system by a significant amount. Throughout this section, $g_{syn} = 0.1$. We vary g_{gap} between 0 and 0.1. In Section 3.2, we showed the existence and stability of two-cluster states in the absence of gap junction coupling. Figure 3.4.1 displays the simulations done with 20 oscillators when $g_{gap} = 0$. In Figure 3.4.1(a), random initial conditions lead to a solution where half of the oscillators have the same phase and the rest are π apart. There are multiple

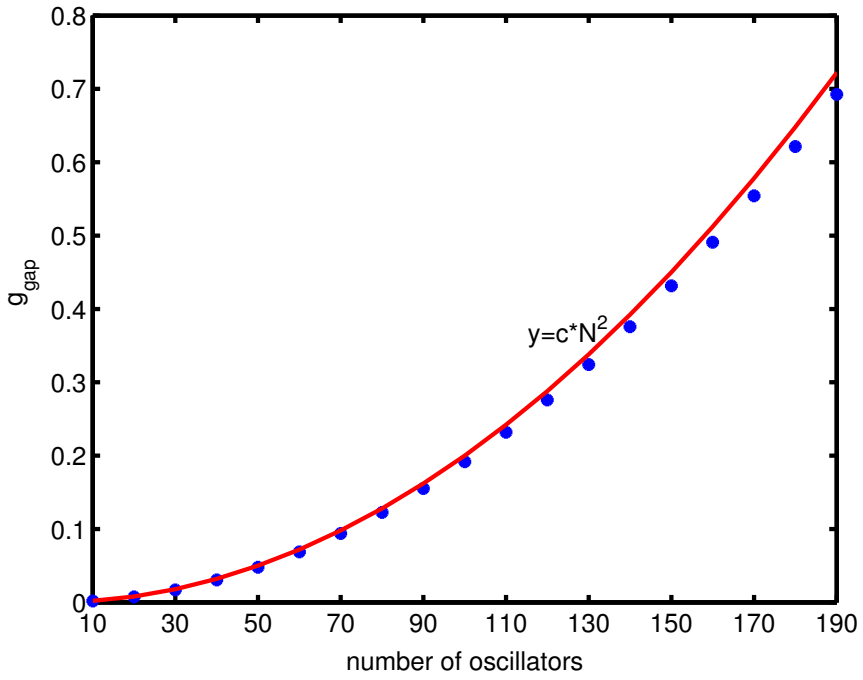

Figure 3.3.1: Relation between g_{gap} and N is shown by the blue $*$'s. The red line is the curve that fits the data with $y = cN^2$ and $c = 0.00002$. g_{syn} is fixed at 0.1 throughout the computation.

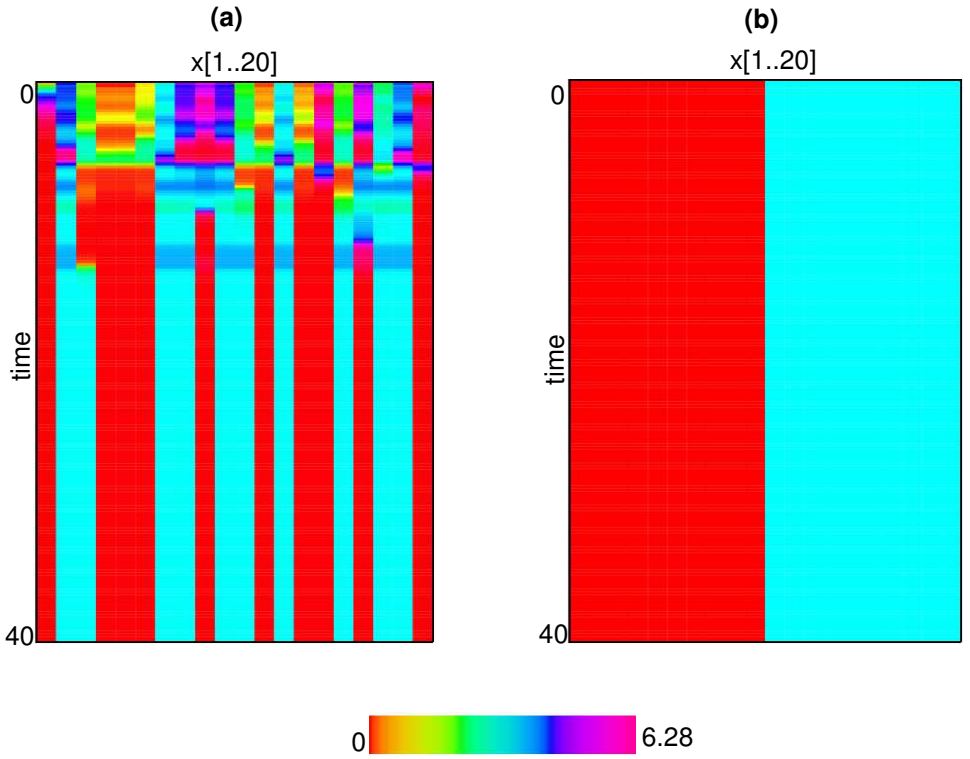

Figure 3.4.1: Two-cluster solution in a network with 20 oscillators where $x_j = \theta_j - \theta_1$.

(a) Random initial conditions converge to a two-cluster solution where the phase difference between oscillators is either 0 or π. The number of oscillators in each cluster is the same.

(b) The two-cluster is solution is represented in this form for convenience.

ways to organize N oscillators in two equal-sized clusters. For computational convenience, we consider the trivial case where the first $N/2$ oscillators are in one cluster and the rest belongs to the other cluster. Such a solution is displayed in Figure 3.4.1(b). The two-cluster solution is stable when there is no gap junction coupling present or when the coupling is weak. Increasing g_{gap} beyond 0.003491 results in a transcritical bifurcation as one of the eigenvalues of the stability matrix crosses over to positive real axes.

When $g_{gap} = 0.1$, there are several stable solutions to the system. One of them is the traveling wave. This solution loses stability as g_{gap} decreases. For $N = 20$, a Hopf bifurcation occurs at $g_{gap} = 0.007463$. To determine the stability of the periodic solutions, we can either compute the coefficients for the normal form or we can use AUTO bifurcation package [12]. Figure 3.4.2 displays the whole bifurcation diagram. There is a region of bistability where we have stable two-cluster state and stable periodic orbits. By perturbing the system enough, we switch between these solutions.

We have seen that the value of g_{gap} where the Hopf bifurcation occurs depends on the size of the network. Figure 3.4.3 is a drawing that shows how the bifurcation diagram changes as N changes. g_c is the value of g_{gap} where the two-cluster state becomes unstable and g_h is where the Hopf bifurcation is observed. We notice that regions of bistability change drastically as N increases.

We now look at the simulations with 10 oscillators. Different from the other simulations we see that there is also a patterned solution when $g_{gap} = 0.1$. In Figure 3.4.4(a), we see a regular traveling wave solution whereas panel (b) displays the plot for the patterned state. Periodic orbits look like zig-zag patterns (panel (c)) and they eventually are replaced by solutions that look like the ones in panel (d). There is another traveling wave solution for

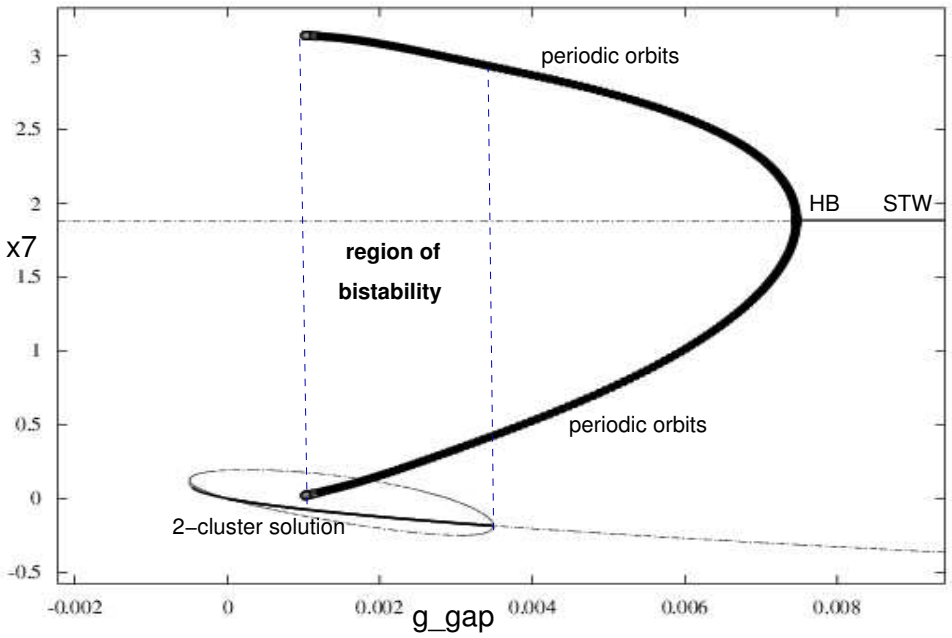

Figure 3.4.2: Bifurcation diagram as g_{gap} varies for a system with 20 oscillators. Two-cluster state becomes unstable at $g_{gap} = 0.003491$. Branch of solutions bifurcating from two-cluster state are drawn. Traveling waves become unstable through a Hopf bifurcation at $g_{gap} = 0.007463$. The periodic orbits are stable and they terminate at a homoclinic point. There is a region where both the two-cluster state and periodic orbits are stable.

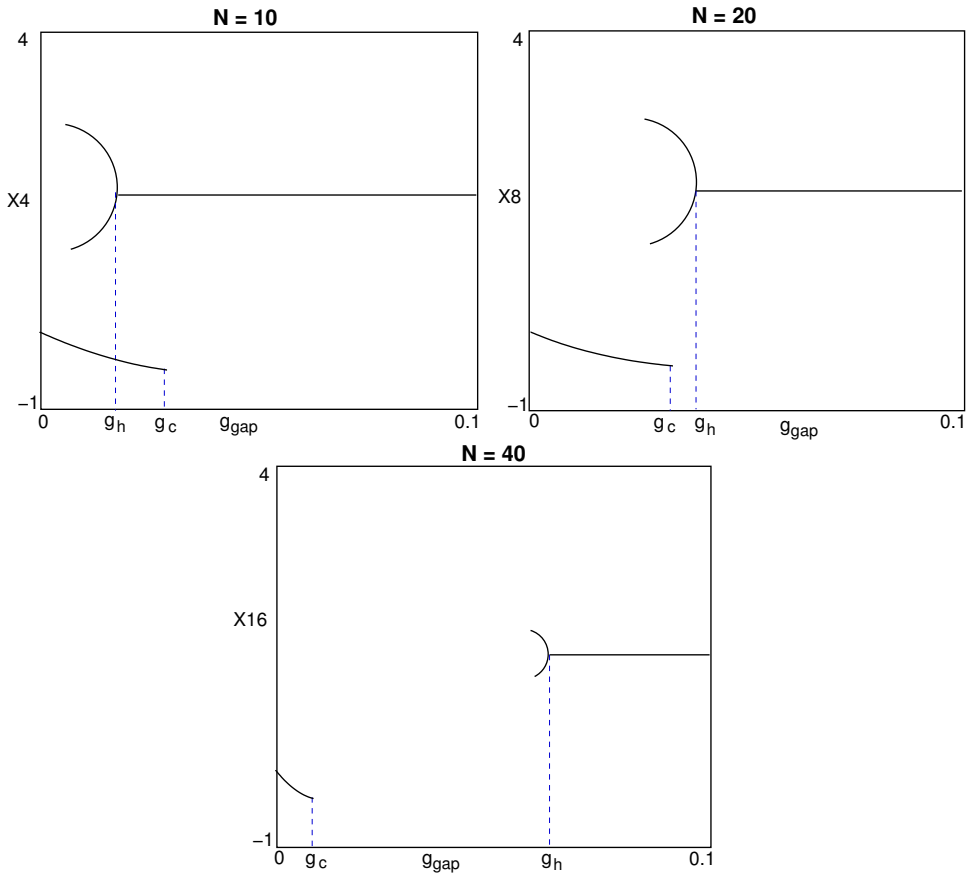

Figure 3.4.3: Sketches of bifurcation diagrams for various N values. g_c is the value of g_{gap} where the two-cluster state becomes unstable and g_h is where the Hopf bifurcation is observed. For $N = 10$, $g_c = 0.02759$, $g_h = 0.001823$; $N = 20$, $g_c = 0.003491$, $g_h = 0.007463$; $N = 40$, $g_c = 0.003771$, $g_h = 0.03045$.

$g_{gap} = 0.01$, where we see two waves in the ring (panel (e)). These become unstable at another Hopf point where g_{gap} is very close to 0. A new pattern of periodic solutions are observed after this point (panel (f)).

Repeating the simulations with other N values, results in similar plots. We note that it is possible to get waves going in both directions (clockwise and counter-clockwise). The periodic zig-zag solutions doesn't change in appearance, but the periodic solutions that we get near the termination of the zig-zag patterns can be different. Figure 3.4.5 contains such solutions where $N = 20$. With more oscillators, it is easier to see that the bifurcation from the double traveling wave results in double zig-zag patterns. Figure 3.4.6 shows the transition from traveling wave to periodic solutions.

3.5 CONCLUSIONS

We studied a system of globally coupled oscillators given in (3.1). Types of solutions possible depends on the coupling function H_{syn}. A widely studied example of such systems is the Kuramoto model where the coupling is sinusoidal. To get the existence of n-cluster states with $n > 1$, one needs to consider a coupling function with higher harmonics. We computed H_{syn} from a biophysical model and used an approximation by considering the dominant Fourier modes. We have seen stable two-cluster states with equal cluster sizes π apart from one another. It was also possible to see some different size clusters with p close to $1/2$. We focused our attention on the previous case.

Previous studies looked at globally coupled phase oscillators with addition of noise. Here

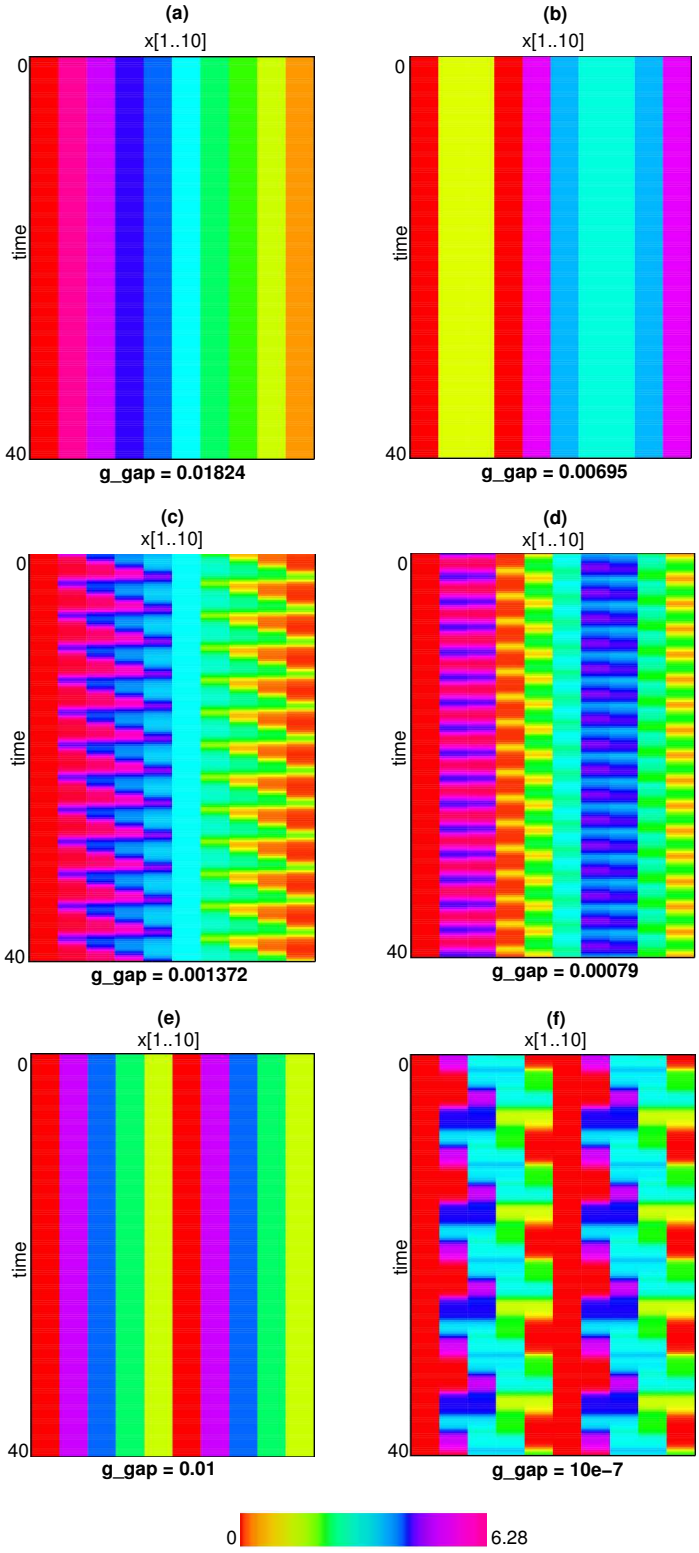

Figure 3.4.4: Different patterns observed are shown in a network with 10 oscillators as $g_{syn} = 0.1$ and g_{gap} varies.

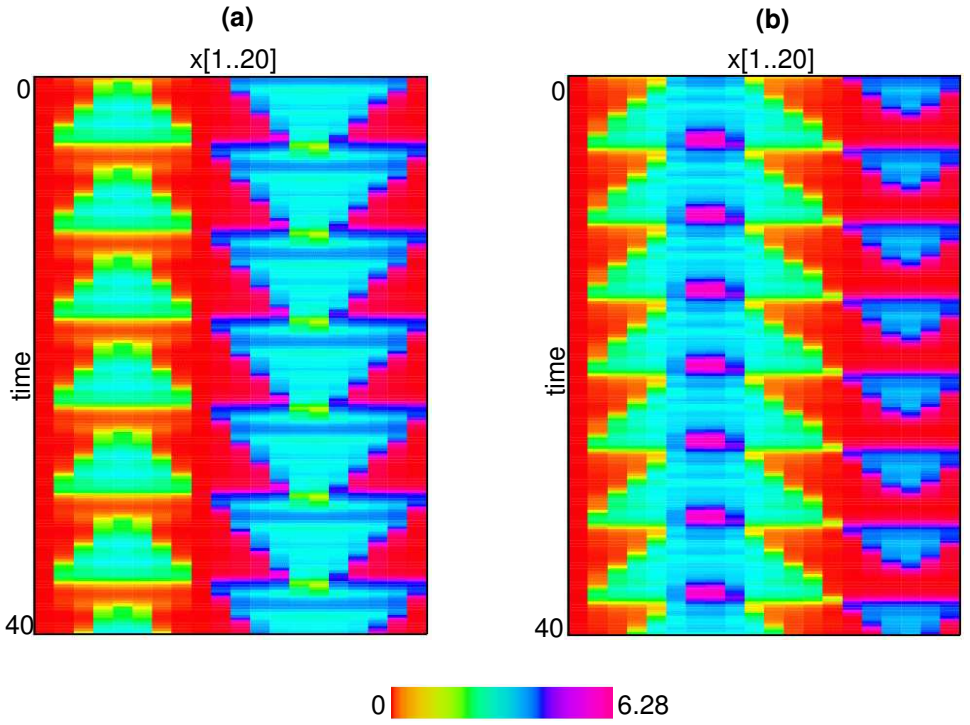

Figure 3.4.5: Before the periodic zig-zag solutions terminate, there is a new pattern observed. For $N = 20$, (a) $g_{gap} = 0.00095$ and (b) $g_{gap} = 0.0011$.

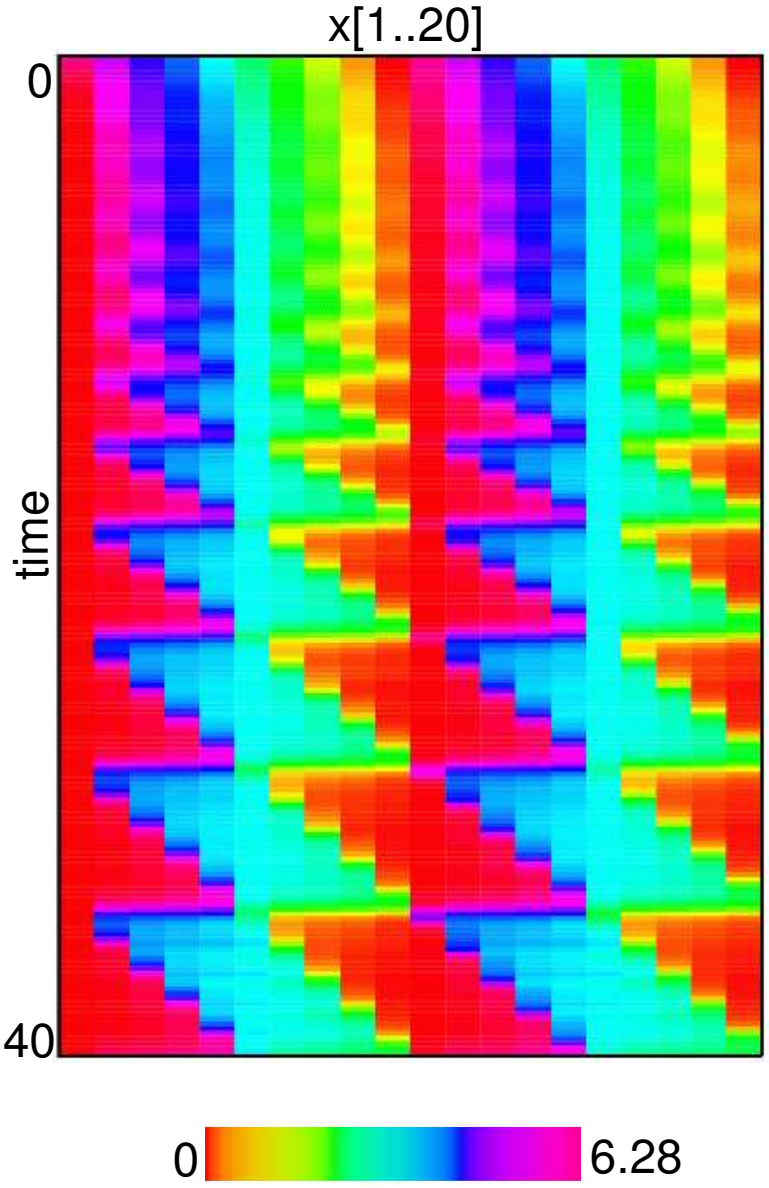

Figure 3.4.6: A double traveling wave solution bifurcates into double zig-zag patterns for $N = 20$ and $g_{gap} = 0.001$.

we took a different path and added local gap junction coupling. Each oscillator was coupled to its nearest neighbors via gap junctions. In pairwise connections, H_{gap} had a synchronizing effect. The overall system behavior changed drastically as we added local gap junctions. Two-cluster state lost its stability as we tuned g_{gap} up and the system produced traveling waves. We found that depending on the network size, the system displayed bistability between the traveling wave and two-cluster solution and/or between the periodic zig-zag solution and two-cluster solution. Changing the network size had drastic effects on network behavior in this rather simple setting. In summary, we were able to analyze a system that has been long studied with a twist and found very interesting behavior. We also want to point out that our work has focused on the interplay of traveling waves and cluster solutions whereas other studies on similar networks analyzed the synchronous solution and clusters of varying sizes [3, 27, 31].

4.0 ASYNCHRONOUS SOLUTION

4.1 INTRODUCTION

Synchronization in populations of interacting elements has been the subject of study in physical, biological, chemical settings. The goal is to find the underlying mechanism that is responsible for collective behavior among the members of the given population. One way of looking at the problem is to consider the elements as phase oscillators and study the phase as time evolves. We demonstrated such examples in the previous chapters. In this chapter, we examine a well-studied model for globally coupled phase oscillators. Kuramoto analyzed a network of phase oscillators coupled through the sine of their phase differences [43]. Without coupling each oscillator runs along the limit cycle attractor with an arbitrary frequency. This model, which is simple yet non-trivial, has been the subject of many studies to this date.

Since our aim is to analyze the effects of chemical and electrical coupling, we will study a variation of the Kuramoto model with local gap junctions. We start this chapter by reviewing the original model. In Section 4.2 we study the stability of asynchronous state in which the phase of oscillators take on values in the interval $[0, 2\pi]$ with equal probability. We calculate the critical coupling strength where the asynchronous state becomes unstable for the original

and noise added systems.

In Section 4.3, we look at a collection of m groups of oscillators with each group consisting of N members. Inside a group, the coupling structure is similar to what we have been studying so far: each oscillator is connected to the rest of the oscillators in the group via a combination of synaptic inhibition and gap junctions. Within groups, we assume each oscillator in the collection is coupled to the rest of the oscillators in the collection via synaptic inhibition and the oscillators in neighboring groups are coupled via gap junctions. Figure 4.1.1 displays an illustration of the network structure. We will study the stability of asynchronous state as the coupling strength and noise in the system changes. We present our numerical results in this section along with the analytical findings.

4.2 THE KURAMOTO MODEL

Collective synchronization can be seen in biological or physical examples such as flashing fireflies, pacemaker cells in the heart and arrays of lasers. Winfree proposed that synchronization can be studied in large networks of interacting limit-cycle oscillators where the coupling between oscillators is weak [60]. His ideas were later used by Kuramoto to come up with a general form for the dynamics of almost identical weakly coupled limit-cycle oscillators. Kuramoto's model can be written down generally as follows:

$$\dot{\theta_j} = \omega_j + \sum_{k=1}^{N} K_{jk}(\theta_k - \theta_j), \quad \text{j=1}, \ldots, N \tag{4.1}$$

where the dynamics of each oscillator is given by the phase of the oscillator , θ_j. ω_j is the natural frequency of oscillator j. The frequencies ω_j are constant in time and distributed

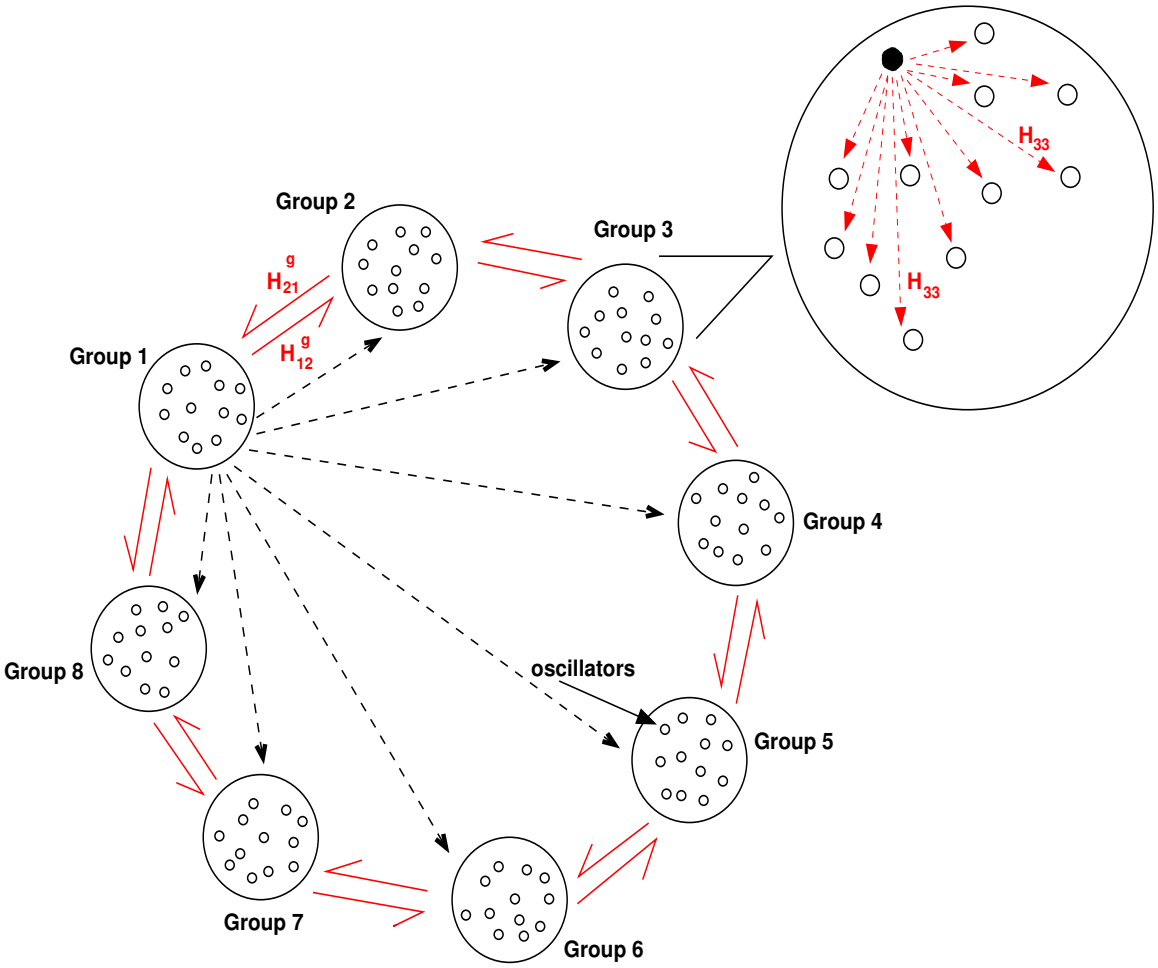

Figure 4.1.1: An illustrative figure of a collection of oscillators organized in $m = 8$ groups. Each group consists of $N = 12$ oscillators. The red solid arrows represent the gap junction coupling between groups, i.e, each oscillator in Group 1 is connected to each oscillator in Group 2 and Group 3. The synaptic coupling is global in the sense that each oscillator in the collection is coupled to the rest of the oscillators in the collection (black dashed lines represent the synaptic coupling). Within each group the synaptic and gap junction coupling is represented by a function H_{jj} for $j = 1, 2, .., 8$ (red dashed lines represent this combination coupling).

according to some probability density $g(\omega)$. Without loss of generality we assume that $g(\omega)$ is symmetric about the mean value 0. The form of coupling taken by Kuramoto is $K_{jk} = \frac{K}{N}\sin(\theta k - \theta j)$. Using mean-field theory, we can analyze the system. The complex order parameter r is defined as

$$re^{i\psi} = \frac{1}{N}\sum_{k=1}^{N} e^{i\theta_k} \tag{4.2}$$

Multiplying both sides by $e^{-i\theta_j}$ and taking the imaginary parts results in

$$r\sin(\psi - \theta_j) = \frac{1}{N}\sum_{k=1}^{N}\sin(\theta_k - \theta_j)$$

Thus, the Kuramoto model can be written as

$$\dot{\theta_j} = \omega_j + Kr\sin(\psi - \theta_j) \tag{4.3}$$

where Kr is the mean-field strength and ψ is the mean phase. If r is independent of time, solving (4.3) and substituting the solutions in (4.2) gives us a self-consistent equation for r. This tells us that there is a phase transition at some critical value of the coupling strength. The order parameter is zero for $K < K_c$ and becomes nonzero afterwards. Macroscopic oscillations are seen after the transition point. They are later entrained to one collective oscillation. In other terms, there is a critical value of the coupling strength below which the asynchronous state is stable and later as we increase K, the oscillators are synchronized and r approaches 1. Kuramoto's original analysis uses the self consistency condition for r and an assumption about the distribution to solve for K_c. The reader is referred to review papers for details of Kuramoto's original derivation and other approaches [1, 53].

We will give the derivation using Strogatz's approach of using a probability density function $\rho(\theta, \omega, t)$ in the limit of infinitely many oscillators. For each natural frequency ω,

we imagine a continuum of oscillators distributed on the circle. Let $\rho(\theta, \omega, t)d\theta$ to denote is the fraction of oscillators with phase that lies in the interval $[\theta, \theta + d\theta]$. The equation for the order parameter given in (4.2) can be written as an average over phase and frequency

$$re^{i\psi} = \int_0^{2\pi} \int_{-\infty}^{\infty} e^{i\theta} \rho(\theta, \omega, t) g(\omega) d\omega d\theta. \tag{4.4}$$

ρ is non-negative, 2π-periodic in θ and satisfies the normalization condition

$$\int_0^{2\pi} \rho(\theta, \omega, t) d\theta = 1 \tag{4.5}$$

for all values of the natural frequency ω and t. Note that the oscillators move with velocity

$$v(\theta, \omega, t) = \omega + Kr \sin(\psi - \theta). \tag{4.6}$$

We derive a continuity equation for the oscillator density by

$$\frac{\partial \rho}{\partial t} + \frac{\partial}{\partial \theta}(\rho v) = 0 \tag{4.7}$$

Using (4.4) and (4.6), (4.7) can be written as:

$$\frac{\partial \rho}{\partial t} = \frac{\partial}{\partial \theta} \left[\rho \left(\omega + K \int_0^{2\pi} \int_{-\infty}^{\infty} \sin(\theta' - \theta) \rho(\theta', \omega', t) g(\omega') d\omega' d\theta' \right) \right] \tag{4.8}$$

This equation is the continuum limit for the Kuramoto model. We will study the existence and stability of asynchronous solution for the Kuramoto model using (4.8). Asynchronous solution is the case where each phase in $[0, 2\pi]$ is taken by the oscillators with same probability. In this case $r = 0$ and $\rho = 1/2\pi$. Substituting ρ in (4.8) we see that this is indeed a solution to the Kuramoto model. Next, we study the stability of this solution. Let

$\rho(\theta,\omega,t) = \frac{1}{2\pi} + \nu(\theta,\omega,t)$ in (4.7) where ν is a small perturbation from the asynchronous solution. We study the linear stability problem by neglecting the nonlinear terms in ν

$$\frac{\partial \nu}{\partial t} = -\frac{\partial}{\partial \theta}\left[\omega\nu + \frac{K}{2\pi}\int_{-\infty}^{\infty} g(\omega)d\omega \int_0^{2\pi} \nu(\phi,\omega,t)\sin(\phi-\theta)d\phi\right] \tag{4.9}$$

Solutions to (4.9) are of the form $\nu(\theta,\omega,t) = e^{\lambda t}\Psi(\omega)e^{i\theta}$.

Substituting this into (4.9) gives us

$$\begin{aligned} \lambda\Psi(\omega)e^{i\theta}e^{\lambda t} &= -i\omega\Psi(\omega)e^{i\theta}e^{\lambda t} \\ &\quad + \frac{K}{2\pi}\int_{-\infty}^{\infty} g(\omega)d\omega \int_0^{2\pi} e^{i\theta}e^{\lambda t}\Psi(\omega)\cos(\phi-\theta)d\phi \end{aligned} \tag{4.10}$$

Canceling $e^{\lambda t}$ from both sides of the equation and letting $\phi' = \phi - \theta$, we rewrite (4.10) as

$$\lambda\Psi(\omega)e^{i\theta}e^{\lambda t} = -i\omega\Psi(\omega)e^{i\theta}e^{\lambda t} + \frac{K}{2\pi}e^{i\theta}e^{\lambda t}\int_{-\infty}^{\infty}\Psi(\omega)g(\omega)d\omega\int_{-\theta}^{2\pi-\theta} e^{i\phi'}\cos(\phi')d\phi'$$

We can now cancel out $e^{i\theta}$. Note that $\int_{-\theta}^{2\pi-\theta} f(\phi)d\phi = \int_0^{2\pi} f(\phi)d\phi$ for a 2π-periodic function f. The final form of the equation is:

$$\lambda\Psi(\omega) = -i\omega\Psi(\omega) + \frac{K}{2\pi}\int_{-\infty}^{\infty}\Psi(\omega)g(\omega)d\omega\int_0^{2\pi} e^{i\phi'}\cos(\phi')d\phi' \tag{4.11}$$

Noticing that $\int_0^{2\pi} e^{i\phi'}\cos(\phi')d\phi' = \pi$ and letting $A = \int_{-\infty}^{\infty}\Psi(\omega)g(\omega)d\omega$, we rewrite (4.11) as:

$$\lambda\Psi(\omega) = -i\omega\Psi(\omega) + \frac{K}{2}A$$

Solving for $\Psi(\omega)$ gives us the equation

$$\Psi(\omega) = \frac{K}{2}\frac{A}{(\lambda + i\omega)}$$

Substituting $\Psi(\omega)$ in the equation for A, we now can write

$$\begin{aligned} A &= \int_{-\infty}^{\infty} g(\omega)\frac{KA}{2(\lambda + i\omega)}d\omega \\ \Leftrightarrow 1 &= \frac{K}{2}\int_{-\infty}^{\infty}\frac{g(\omega)}{\lambda + i\omega}d\omega \end{aligned}$$

If we take $g(\omega)$ to be even and unimodal, we see that there is at most one solution for λ which is real when exists. We write the last equation as

$$\begin{aligned} 1 &= \frac{K}{2}\int_{-\infty}^{\infty}\frac{g(\omega)(\lambda - i\omega)}{\lambda^2 + \omega^2}d\omega \\ \Leftrightarrow 1 &= \frac{K}{2}\int_{-\infty}^{\infty}\frac{\lambda g(\omega)}{\lambda^2 + \omega^2}d\omega - i\frac{K}{2}\int_{-\infty}^{\infty}\frac{\omega g(\omega)}{\lambda^2 + \omega^2}d\omega \end{aligned}$$

and note that the second integral in the last equation is zero. The final form of the equation is

$$1 = \frac{K}{2}\int_{-\infty}^{\infty}\frac{\lambda g(\omega)}{\lambda^2 + \omega^2}d\omega \tag{4.12}$$

Equation (4.12) implies that the eigenvalue $\lambda \geq 0$ so the asynchronous state is not linearly stable. For values of $\lambda \to 0^+$ the integral $\int_{-\infty}^{\infty}\frac{\lambda g(\omega)}{\lambda^2+\omega^2}d\omega \to \pi g(0)$, so we recover the value of the critical coupling strength, K_c, found by Kuramoto in the form

$$1 = \frac{1}{2}K_c\pi g(0) \tag{4.13}$$

Strogatz proves the neutral stability of the asynchronous solution using this method in his paper with Mirollo [54]. Sakaguchi also studied the Kuramoto model and its extension by allowing fluctuations in natural frequencies [51].

Here is the equation governing the phase changes:

$$\dot{\theta}_i = \omega_i + \xi_i(t) + \frac{K}{N}\sum_{j=1}^{N}\sin(\theta_j - \theta_i) \tag{4.14}$$

where ξ_i's are white noise processes with zero mean and σ^2 as power spectral density. We use similar analysis as before to write down the continuity equation

$$\frac{\partial \rho}{\partial t} = \frac{\sigma^2}{2}\frac{\partial^2 \rho}{\partial \theta^2} - \frac{\partial}{\partial \theta}(\rho\nu) \tag{4.15}$$

After these modifications, the results given earlier change slightly

$$\lambda\bar{\Psi(\omega)} = -i\omega\Psi(\omega) + \frac{K}{2}A - \frac{\sigma^2}{2}\Psi(\omega)$$

Let $D = \sigma^2/2$, and solve for $\Psi(\omega)$

$$\Psi(\omega) = \frac{K}{2}\frac{A}{\lambda + i\omega + D}$$

Substitute this into the equation for A to get

$$\begin{aligned} A &= \frac{K}{2}\int_{-\infty}^{\infty}\frac{A}{\lambda + i\omega + D}g(\omega)d\omega \\ \Leftrightarrow 1 &= \frac{K}{2}\int_{-\infty}^{\infty}\frac{g(\omega)}{(\lambda + D + i\omega)}d\omega \end{aligned} \tag{4.16}$$

Solutions to (4.16) are the eigenvalues for the linear stability problem for the Kuramoto model with noise. When random noises are added, the mutual entrainment (synchronization) becomes less clear. Thus, the random noises make the critical coupling strength K_c larger without any quantitative change with respect to phase transition. For further details on the calculations, the reader is referred to [54, 9, 51].

4.3 KURAMOTO MODEL WITH GAP JUNCTIONS

In this section, we extend the Kuramoto model to allow for local coupling between oscillators. We consider a network of mN oscillators organized in m groups with each group consisting of N oscillators. The oscillators are globally coupled via synaptic inhibition. The gap junction coupling is local in the sense that each oscillator is connected to other oscillators in the nearest neighbor groups and the group to which it belongs. So each oscillator makes $3N$ electrical synapses (see Figure 4.1.1). For $m = 2, 3$, the coupling is all:all. For $m > 3$, we write down a set of equations for the network:

$$\frac{d\theta_j^i}{dt} = \xi_j^i(t) + \frac{1}{N}\sum_{l=1}^{N}\left(\sum_{k=1}^{m} H_{jk}(\theta_k^l - \theta_j^i)\right) \quad \text{i=1,}\ldots,N \quad \text{j=1,}\ldots,m \tag{4.17}$$

where ξ_j^i's are white noise processes with zero mean and σ^2 is the power spectral density, H_{jk}'s are the coupling functions (their form will be given explicitly later in the section). Note that (4.17) differs from the Kuramoto model in the sense that we do not have the arbitrary natural frequencies. Instead, heterogeneity is introduced via the noise process.

As in Section 4.2, we want to study the existence and stability of the asynchronous solution. We will use the probability density approach. Let $\rho(\theta_1, \theta_2, \ldots, \theta_m, t)$ be the probability distribution for oscillators in m groups having phases $\theta_1, \ldots, \theta_m$ at time t. ρ satisfies the normalization condition

$$\int_0^{2\pi} \ldots \int_0^{2\pi} \rho(\theta_1, \theta_2, \ldots, \theta_m, t) d\theta_1 \ldots d\theta_m = 1$$

which is a generalized form of (4.5). ρ is 2π-periodic in its first m arguments. From Sakaguchi's formulation [51], we can write down a Fokker-Planck equation for ρ

$$\begin{aligned}\frac{\partial \rho}{\partial t} &= \frac{\sigma^2}{2}\left(\frac{\partial^2 \rho}{\partial \theta_1^2} + \cdots + \frac{\partial^2 \rho}{\partial \theta_m^2}\right) \\ &\quad - \sum_{j=1}^{m} \frac{\partial}{\partial \theta_j}\left\{\rho(\Theta, t)\int_0^{2\pi}\cdots\int_0^{2\pi}\rho(\Phi, t)\sum_{k=1}^{m} H_{jk}(\theta_k - \theta_j)d\phi_1 \ldots d\phi_m\right\} \end{aligned} \tag{4.18}$$

where $\Theta = (\theta_1, \ldots, \theta_m)$ and $\Phi = (\phi_1, \ldots, \phi_m)$. We define the marginal distribution for θ_i:

$$\rho_i(\theta) = \int_0^{2\pi}\cdots\int_0^{2\pi}\rho(\phi_1, \ldots, \phi_{i-1}, \theta, \phi_{i+1}, \ldots, \phi_m)\prod_{\phi j: j\neq i} d\phi_j$$

Let us illustrate the case where $m = 2$. We rewrite (4.18) as:

$$\begin{aligned}\frac{\partial \rho}{\partial t} &= \frac{\sigma^2}{2}\left(\frac{\partial^2 \rho}{\partial \theta_1^2} + \frac{\partial^2 \rho}{\partial \theta_2^2}\right) \\ &\quad -\frac{\partial}{\partial \theta_1}\left\{\rho(\theta_1, \theta_2)\int_0^{2\pi}\int_0^{2\pi}\rho(\phi_1, \phi_2)\left[H_{11}(\phi_1 - \theta_1) + H_{12}(\phi_2 - \theta_1)\right]d\phi_1 d\phi_2\right\} \\ &\quad -\frac{\partial}{\partial \theta_2}\left\{\rho(\theta_1, \theta_2)\int_0^{2\pi}\int_0^{2\pi}\rho(\phi_1, \phi_2)\left[H_{21}(\phi_1 - \theta_2) + H_{22}(\phi_2 - \theta_2)\right]d\phi_1 d\phi_2\right\}\end{aligned} \tag{4.19}$$

Integrating both sides of the equation (4.19) with respect to θ_1 and θ_2 and using the definitions for marginals, we can write (4.19) as a system of two partial differential equations:

$$\begin{aligned}\frac{\partial \rho_1(\theta_1)}{\partial t} &= \frac{\sigma^2}{2}\frac{\partial^2 \rho_1(\theta_1)}{\partial \theta_1^2} - \frac{\partial}{\partial \theta_1}\left[\rho_1(\theta_1)\int_0^{2\pi}\rho_1(\phi_1)H_{11}(\phi_1 - \theta_1)d\phi_1\right] \\ &\quad -\frac{\partial}{\partial \theta_1}\left[\rho_1(\theta_1)\int_0^{2\pi}\rho_2(\phi_2)H_{12}(\phi_2 - \theta_1)d\phi_2\right]\end{aligned}$$

$$\begin{aligned}\frac{\partial \rho_2(\theta_2)}{\partial t} &= \frac{\sigma^2}{2}\frac{\partial^2 \rho_2(\theta_2)}{\partial \theta_2^2} - \frac{\partial}{\partial \theta_2}\left[\rho_2(\theta_2)\int_0^{2\pi}\rho_1(\phi_2)H_{21}(\phi_1 - \theta_2)d\phi_1\right] \\ &\quad -\frac{\partial}{\partial \theta_2}\left[\rho_2(\theta_2)\int_0^{2\pi}\rho_2(\phi_2)H_{22}(\phi_2 - \theta_2)d\phi_2\right]\end{aligned}$$

Let's define $H_{11} = H_{22} \equiv H$ and $H_{12} = H_{21} \equiv G$ so that H is the function representing interactions within a group and G represents interactions between groups. Two solutions to the system given can be characterized as follows:

- $\rho_1(\theta) = \rho_2(\theta) \quad \Rightarrow$ Group 1 and Group 2 are in-phase synchronized
- $\rho_1(\theta) = \rho_2(\theta - \pi) \quad \Rightarrow$ Group 1 and Group 2 are anti-phase synchronized

In order to study the existence and stability of the asynchronous state, we write down the system given above in the following form

(4.20)
$$\frac{\partial \rho_j(\theta,t)}{\partial t} = \frac{\sigma^2}{2}\frac{\partial^2 \rho_j}{\partial \theta^2} - \frac{\partial}{\partial \theta}\left\{\rho_j(\theta)\left[\int_0^{2\pi} \rho_j(\phi)H_{jj}(\phi-\theta)d\phi + \int_0^{2\pi} \rho_k(\phi)H_{jk}(\phi-\theta)d\phi\right]\right\}$$

for $j = 1, 2$. Note that the derivation of these equations for $m > 2$ is similar. It is easy to see that $\rho_j(\theta) = 1/2\pi$ is a solution to (4.20). We take a perturbation of the asynchronous solution, $\rho_j(\theta,t) = \frac{1}{2\pi} + \nu_j(\theta,t)$, and write the equation for the linear stability problem excluding nonlinear terms

(4.21)
$$\begin{aligned}\frac{\partial \nu_j}{\partial t} &= \frac{\sigma^2}{2}\frac{\partial^2 \nu_j}{\partial \theta^2} - \frac{\partial}{\partial \theta}\left[\nu_j(\theta_2)\{\bar{H_{jj}} + \bar{H_{jk}}\}\right] \\ &\quad -\frac{\partial}{\partial \theta}\left[\frac{1}{2\pi}\int_0^{2\pi} H_{jj}(\phi-\theta)\nu_j(\phi) + H_{jk}(\phi-\theta)\nu_k(\phi)\right]\end{aligned}$$

where $\bar{H_{jj}}$ and $\bar{H_{jk}}$ are the average values of the coupling functions over a period. The solutions to (4.21) are of the form $\nu_j = e^{\lambda t}e^{in\theta}\mathbf{v_j}$ where $\mathbf{v_j}$ is a constant. Substituting ν_j into (4.21) and using the information about the periodicity of the functions H_{jk}, we get an equation for the eigenvalue λ

$$\lambda \mathbf{v_j} = -\frac{\sigma^2 n^2}{2}\mathbf{v_j} - in\Omega_j \mathbf{v_j} + \frac{1}{2\pi}\int_0^{2\pi}\sum_{k=1}^{m} H'_{jk}(\phi)\mathbf{v_k}e^{in\phi}d\phi$$

where $\Omega_j = \sum_k \bar{H_{jk}}$. If the coupling functions satisfy $H_{jk} = H_{j-k} \pmod m$, the eigenvalue problem can be rewritten as

(4.22)
$$\lambda_n \mathbf{v_j} = -(in\Omega_j + \frac{\sigma^2 n^2}{2})\mathbf{v_j} + \sum_{k=0}^{m-1}\alpha_{j-k}(n)\mathbf{v_k}$$

where

$$\alpha_{j-k}(n) = \frac{1}{2\pi}\int_0^{2\pi} H'_{jk}(\phi)e^{in\phi}d\phi$$

is the nth complex Fourier term for the function H'_{jk}. If we were to write this equation as a linear system $\lambda\mathbf{v} = A\mathbf{v}$, the matrix A has a special structure. It is a circulant matrix and the eigenvectors have the following form:

$$\mathbf{v}^T = [1\ e^{2\pi ij/m} \dots e^{2\pi i(m-1)j/m}]^T$$

Thus, we derive the equation for the eigenvalues as

$$\lambda_n = -in\Omega - \frac{n^2\sigma^2}{2} + \hat{\alpha}(l,n)$$

with $\hat{\alpha}(l,n) = \sum_{k=0}^{m-1}\alpha_k(n)e^{2\pi kl/m}$. If we look at the real parts of the eigenvalues, we see that the stability of the asynchronous solution depends on the interplay between the noise strength and the harmonic terms for the coupling function.

We now present some simulation results with 600 oscillators. The oscillators are divided into 6 groups with equal size and the coupling structure is described above. We chose a simple form for the coupling functions: global coupling function is chosen as $-\sin(x)$ and local coupling is $k\sin(x)$ where k is a positive coupling strength. Figure 4.3.1 displays the results of the simulations where actual phases of the oscillators are plotted in time. In panel (a), we see that asynchrony is a solution in the absence of gap junction coupling. By adding small amounts of gap junctions ($k \neq 0$), we see the emergence of a traveling wave-like solution where the oscillators in in the same group tend to synchronize to the same phase while preserving a phase difference among different groups (panel (b)). Increasing the gap junction coupling strength makes this pattern more visible (panel (c)). In panel (d), we present the case with no noise added where we get a regular traveling wave solution.

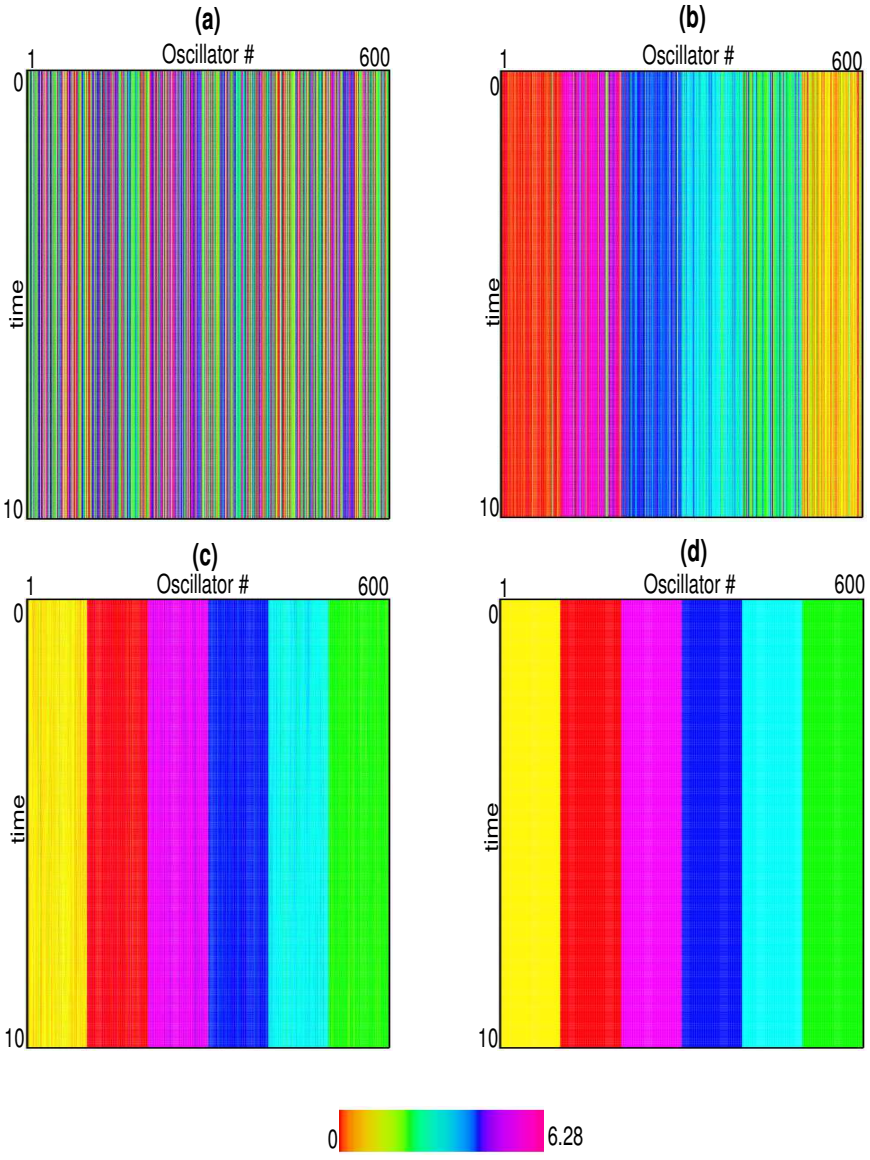

Figure 4.3.1: A network of 600 oscillators organized in 6 equisized groups. (a) Asynchronous solution with $D = \sigma^2/2 = 0.05$ and $k = 0$, (b) Gap junction coupling disrupts the asynchronous solution, $k = 0.01$, (c) for $k = 0.04$ the traveling wave like solution becomes more visible, (d) traveling wave solution with no noise and $k = 0.04$.

4.4 CONCLUSIONS

In this chapter, we have studied one of the most widely studied models for globally coupled oscillators. Since the time the Kuramoto model was introduced in 1975, there have been many papers published about the model and its extensions. Despite the simple form of the model, it displays rich behavior and there are still open problems related to the model.

We first reviewed the Kuramoto model and its version with added noise. We looked at the linear stability problem for the asynchronous solution. The original model lacks spatial structure. By adding local gap junctions, we saw that the asynchronous state loses stability and traveling wave solutions emerge. In the original model, the asynchronous state becomes unstable as the coupling strength increases and the oscillators become synchronous or partially synchronous. We don't see synchrony in our case but the gap junction coupling helps synchronize the oscillators belonging to the same group and create a phase difference with the other groups.

This chapter is still work in progress and we will continue to study this case in depth.

5.0 DISCUSSION

In this thesis, we examine a network of phase oscillators coupled through electrical and chemical synapses. We study how each type of coupling effects the stability of synchrony, clustered state and asynchrony.

In the first chapter, we study the synchronous solution. Our work is inspired by earlier studies done with Limax where traveling waves were observed without a frequency gradient. We use a phase model to represent the interactions between oscillators. The electrical and chemical synapses have counter acting effects on synchrony. Global inhibition supports anti-phase synchrony and local gap junctions promote in-phase synchrony when a pair of identical oscillators are considered. In the absence of synaptic inhibition, the system is synchronized with no phase lag, but as the strength of the synapses increase there is a bifurcation to a state where there is a localized stable pattern of activity is observed. We derive the normal form equation for the bifurcation. Further increasing the coupling strength results in another bifurcation where the intermediate state transitions to the traveling wave. This traveling wave solution exists and is stable for all values of the parameters. Our numerical results support the analytical results found in this chapter and we are able to explain the existence of traveling waves in a seemingly homogeneous, symmetric system.

In the second chapter, we study the clustered solutions where the oscillators are divided

into subgroups with similar activity patterns. The model we consider is similar in structure to the model in the first chapter with very few modifications. We specifically look at the two-cluster state where half of the oscillators have the same phase and they differ by the same amount from the rest of the oscillators. This solution is stable when there is no gap junction coupling, and loses stability with the addition of even a small amount. Since we know the existence of traveling wave solutions from the previous chapter, we look for them here. We see that the traveling wave solution becomes unstable via a Hopf bifurcation. We compute the bifurcation diagrams for various network sizes. The system exhibits bistability depending on the network size.

In the last chapter, we look at a modified version of the Kuramoto model where we allow for local coupling. We go over the Kuramoto model and study the existence and stability of asynchronous solution. We see that the asynchronous solution loses stability and again the network goes to a traveling wave solution. This is different than the outcome with the original Kuramoto model where synchronous solution emerges as the coupling strength increases.

In this work, we have seen that inhibition and gap junction coupling do not necessarily have a complementary effects on network behavior of coupled oscillators. We have observed that addition of local gap junctions enrich the dynamics of a symmetric globally coupled network with synaptic coupling. Gap junctions support the emergence of traveling waves. We have looked at the problem from three different perspectives and traveling wave behavior was dominant in each of them. We have shown that pattern formation can be observed even in a network with a simple architecture.

APPENDIX A

A.1 PHASE MODEL AND AVERAGING

We study the effects of electrical and chemical coupling in a network of phase oscillators. The phase model we study in Chapter 2 is derived from a biophysical model. Since we will use this reduction throughout the thesis, we state the theorems that enable us to proceed this way. The first theorem was proven by Art Winfree and John Guckenheimer in 1970s and it has been implemented by many researchers since then [25, 28, 34, 43, 47].

Theorem 4 *Phase Model*

Let the following equation

$$\dot{\mathbf{X}} = F(\mathbf{X}), \quad \mathbf{X} \in \mathbb{R}^m \tag{A.1}$$

represent a dynamical system which has an exponentially stable limit cycle $\gamma \in \mathbb{R}^m$ with period 2π so that every trajectory $\hat{\gamma}$ with an initial point $\hat{\gamma(0)}$ in a small neighborhood of γ stays in that neighborhood as $t \to \infty$. Then, the dynamical system given by

$$\dot{\theta} = 1, \quad \theta \in \mathbb{S}^1 \tag{A.2}$$

is a canonical model for all systems that are represented by (A.1).

Proof of this theorem can be found in [34]. A model is canonical if there is a continuous change of variables that transforms any other model from the family into this one [34]. The use of canonical models has many advantages. First, these models are simpler than the original dynamical system. We can derive the canonical model even when F is not given explicitly. The only requirement is that the system has a limit cycle attractor. We have to keep in mind that these models only tell us the local behavior. In order to get global information, one needs to use other tools.

Since we are studying coupled oscillators we need a modified version of Theorem 4. There are several types of coupling: pulsatile, strong and weak. In the case of weak coupling, the system can be written as:

$$\dot{X}_i = F_i(X_i, \lambda) + \epsilon G_i(X, \lambda, \rho, \epsilon), \quad \text{i}=1, \ldots, n \tag{A.3}$$

where ϵ is small enough. Assume that there is a value of the parameter λ such that the uncoupled system

$$\dot{X}_i = F_i(X_i, \lambda), \quad X_i \in \mathbb{R}^n \tag{A.4}$$

has a stable limit cycle attractor $\gamma_i \in \mathbb{R}^n$. As we showed in Theorem (4), we can describe the activity on the limit cycle in terms of the phase $\theta \in \mathbb{S}^1$ of oscillation

$$\dot{\theta}_i = \Omega_i(\lambda)$$

where Ω_i is the natural frequency of the oscillations. Similarly, we can define the behavior of the coupled system with:

$$\dot{\theta}_i = \Omega_i(\lambda) + \epsilon g_i(\theta, \lambda, \rho, \epsilon), \quad \text{i}=1, \ldots, n$$

The latter has been proven using different approaches over the years. Winfree used phase response curves and Malkin's theorem uses the Fredholm Alternative to solve the adjoint problem. We will only discuss Malkin's method here.

Theorem 5 *Malkin's Theorem for Weakly Coupled Oscillators*

Consider the weakly coupled system

$$\dot{X}_i = F_i(X_i) + \epsilon G_i(X), \quad texti = 1, \ldots, n$$

where the uncoupled system ($\epsilon = 0$) has stable 2π-periodic limit cycle solutions $\gamma_i \in \mathbb{R}^n$. Let $\tau = \epsilon t$ be slow time and let $\phi_i(\tau) \in \mathbb{S}^1$ be the phase deviation from the natural oscillation $\gamma_i(t)$, $t \geq 0$. The vector of phase deviations $\phi = (\phi_1, \ldots, \phi_n)^T \in T^n$ is a solution to

$$\phi_i' = H_i(\phi - \phi_i, \epsilon), \quad i=1, \ldots, n$$

where $' = d/d\tau$, the vector $\phi - \phi_i = (\phi_1 - \phi_i, \ldots, \phi_n - \phi_i)^T$ and the function

$$H_i(\phi - \phi_i, 0) = \frac{1}{2\pi} \int_0^{2\pi} Q_i(t)^T G_i(\gamma(t + \phi - \phi_i)) dt$$

where $Q_i(t) \in \mathbb{R}^n$ is the unique non-trivial 2π- periodic solution to the system

$$Q_i' = -\left\{DF_i(\gamma_i(t))\right\} Q_i$$

satisfying the normalization condition $Q_i(0)^T F_i(\gamma_i(0)) = 1$.

Weak coupling allows us to use the method of averaging to reduce the model to a system of phase equations. In this approach, each oscillator is represented by a single variable, *phase*, that lies on $\mathbb{S}^1$. Interactions between two connected oscillators depends on the difference of phases.

A.2 BIOPHYSICAL MODEL AND COUPLING FUNCTIONS

We use the biophysical model given in [13]. Each uncoupled bursting cell in the Limax model has the form:

$$\begin{aligned} C\frac{dV}{dt} &= -I_L - I_K - I_{Ca} \\ &= -g_L(V - E_L) - g_K n^4 (V - E_K) - g_{Ca} m^2 h (V - E_{Ca}) \end{aligned}$$

where n, h obey the equations:

$$\begin{aligned} \frac{dn}{dt} &= .075[a_n(V)(1-n) - b_n(V)n] \\ \frac{dh}{dt} &= 1.125(h_\infty(V) - h)/\tau_h(V) \end{aligned}$$

with

$$\begin{aligned} a_n(V) &= .032(-48 - V)/(\exp(-(48+V)/5) - 1) \\ b_n(V) &= .5\exp(-(43+V)/40) \\ h_\infty(V) &= 1/(1+\exp((V+86)/4)) \\ \tau_h(V) &= \text{if } (V < (-80)) \\ &\quad \text{then } (\exp((V+470)/66.6)) \\ &\quad \text{else } (28 + \exp((V+25)/-10.5)) \end{aligned}$$

The activation gate for the T-type calcium current has the form:

$$m(V) = 1/(1+\exp(-(V+60)))$$

The parameters are $C = 2.66$, $g_K = 5$, $g_L = 0.024$, $g_{Ca} = 2$, $E_K = -90$, $E_{Ca} = 140$, $E_L = -82$, and $E_{syn} = -78$.

Using this model in XPPAUT [22], we compute one full cycle of the periodic orbit. Once we have a nice periodic orbit, we use the Averaging tool under Numerics menu to compute the adjoint. The adjoint is then used by XPPAUT to get the interaction functions. We take the dominating terms which are usually the first 2 or 3 terms that appear in the Data Viewer. For detailed examples, the reader is referred to the manual for XPPAUT [22].

In our case, the approximations of coupling functions are as follows:

$$H_{syn}(x) = 35 + 200\cos(x) + 32\cos(2x) - 95\sin(x) - 5\sin(2x)$$

$$H_{gap}(x) = 87 - 50\cos(x) - 37\cos(2x) + 295\sin(x) - 65\sin(2x)$$

APPENDIX B

To calculate the normal form for the bifurcation, we match the "ϵ" terms from (2.12):

$$\Omega_1 = \int_0^{2\pi} A_1(y') \, [\psi_1(x - y') - \psi_1(x)] \, dy' \equiv \mathcal{L} \, \psi_1$$

We integrate both sides of the equation with respect to x to get $\Omega_1 = 0$. If we solve $\mathcal{L}\psi_1 = 0$, we get that $\psi_1(x) = ze^{ix} + \bar{z}e^{-ix}$ without loss of generality. Next, we look at ϵ^2terms

$$\begin{aligned} \Omega_2 &= \mathcal{L} \, \psi_2 + \int_0^{2\pi} A_2(y') \, [\psi_1(x - y') - \psi_1(x)]^2 \, dy' \\ &\quad + \frac{g_1 \alpha_1}{2\pi} \int_0^{2\pi} [\psi_1(x - y') - \psi_1(x)] \, dy' \end{aligned} \tag{B.1}$$

Substitute ψ_1 in the above equation and multiply both sides of the equation by **1** and integrate w.r.to x

$$\begin{aligned} \int_0^{2\pi} \Omega_2 \, dx &= 8\pi \, z \, \bar{z} \, [B_0(A_2) - B_1(A_2)] \\ \Omega_2 &= 4z \, \bar{z} \, [B_0(A_2) - B_1(A_2)] \end{aligned}$$

where $B_n(A_j) = \int_0^{2\pi} A_j(y')\ e^{\pm iny'}\ dy'$, $j = 1, 2, 3$. Now, we multiply (B.1) by e^{-ix}

$$0 \ = \ -2\pi\ g_1\ \alpha_1\ z$$

which implies $g_1 = 0$. So, we can write $g_{syn} = g^*_{syn} + \epsilon^2 g_2$ and we solve for ψ_2

$$0 \ = \ \mathcal{L}\ \psi_2 + (z^2 e^{2ix} + \bar{z}^2 e^{-2ix})\ [B_2(A_2) + B_0(A_2) - 2B_1(A_2)] \tag{B.2}$$

We now propose that $\psi_2 = C\ z^2 e^{2ix} + \bar{C}\ \bar{z}^2 e^{-2ix}$ and substitute back in (B.1)

$$\begin{aligned} 0 \ = \ & [B_2(A_1) - B_0(A_1)]\ (C\ z^2 e^{2ix} + \bar{C}\ \bar{z}^2 e^{-2ix}) \\ & + [B(A_2) + B_0(A_2) - 2B_1(A_2)]\ (z^2 e^{2ix} + \bar{z}^2 e^{-2ix}) \end{aligned}$$

Looking at the coefficients of z^2 term gives

$$C \ = \ \frac{2B_1(A_2) - B_2(A_2) - B_0(A_2)}{B_2(A_1) - B_0(A_1)} \tag{B.3}$$

We have to make sure here that the denominator is non-zero. This is easy to see since $B_2(A_1) - B_0(A_1) = 0$ would imply that $g^*_{syn} = \frac{g_S \beta_1 (I_2 - 1)}{\alpha_2}$ which is not true since $g^*_{syn} = \frac{g_{gap} \beta_1 (I_1 - 1)}{\alpha_2}$ and $I_1 > I_2$.

Next, we look at "ϵ^3" terms

$$
\begin{aligned}
\Omega_3 &= \mathcal{L}\ \psi_3 + \int_0^{2\pi} A_3(y')\ [\psi_1(x-y') - \psi_1(x)]^3\ dy' \\
&\quad +2\int_0^{2\pi} A_2(y')\ [\psi_1(x-y')\psi_2(x-y') + \psi_1(x)\psi_2(x)]\ dy' \\
&\quad -2\int_0^{2\pi} A_2(y')\ [\psi_1(x-y')\psi_2(x) + \psi_1(x)\psi_2(x-y')]\ dy' \\
&\quad +\frac{g_2\alpha_1}{2\pi}\ \int_0^{2\pi} [\psi_1(x-y') - \psi_1(x)]\ dy' \qquad \text{(B.4)}
\end{aligned}
$$

Let's look at the terms in (B.4) closely

$$
\begin{aligned}
[\psi_1(x-y') - \psi_1(x)]^3 &= [ze^{ix}e^{-iy'} + \bar{z}e^{-ix}e^{iy'} - ze^{ix} - \bar{z}e^{-ix}]^3 \\
&= z^3e^{3ix}e^{-3iy'} + 3z^2\bar{z}e^{ix}e^{-iy'} + 3z\bar{z}^2e^{-ix}e^{iy'} + \bar{z}^3e^{-3ix}e^{3iy'} \\
&\quad -3z^3e^{3ix}e^{-2iy'} - 3z^2\bar{z}e^{ix}e^{-2iy'} - 6z^2\bar{z}e^{ix} \\
&\quad -6z\bar{z}^2e^{-ix} - 3z\bar{z}^2e^{-ix}e^{2iy'} - 3\bar{z}^3e^{-3ix}e^{2iy'} \\
&\quad +3z^3e^{3ix}e^{iy'} + 3z^2\bar{z}e^{ix}e^{iy'} + 6z^2\bar{z}e^{ix}e^{-iy'} \\
&\quad +6z\bar{z}^2e^{-ix}e^{iy'} + 3z\bar{z}^2e^{-ix}e^{-iy'} + 3\bar{z}^3e^{-3ix}e^{iy'} \\
&\quad -z^3e^{3ix} - 3z^2\bar{z}e^{ix} - 3z\bar{z}^2e^{-ix} - \bar{z}^3e^{-3ix}
\end{aligned}
$$

Let $T = [\psi_1(x-y')\psi_2(x-y') + \psi_1(x)\psi_2(x) - \psi_1(x-y')\psi_2(x) - \psi_1(x)\psi_2(x-y')]$, then

$$
\begin{aligned}
T &= [(ze^{ix}e^{-iy'} + \bar{z}e^{-ix}e^{iy'})(Cz^2e^{2ix}e^{-2iy'} + \bar{C}\bar{z}^2e^{-2ix}e^{2iy'}) \\
&\quad +(ze^{ix} + \bar{z}e^{-ix})(Cz^2e^{2ix} + \bar{C}\bar{z}^2e^{-2ix}) \\
&\quad -(ze^{ix}e^{-iy'} + \bar{z}e^{-ix}e^{iy'})(Cz^2e^{2ix} + \bar{C}\bar{z}^2e^{-2ix}) \\
&\quad -(ze^{ix} + \bar{z}e^{-ix})(Cz^2e^{2ix}e^{-2iy'} + \bar{C}\bar{z}^2e^{-2ix}e^{2iy'}) \\
&= Cz^3e^{3ix}e^{-3iy'} + \bar{C}z\bar{z}^2e^{-ix}e^{iy'} + Cz^2\bar{z}e^{ix}e^{-iy'} \\
&\quad +\bar{C}\bar{z}^3e^{-3ix}e^{3iy'} + Cz^3e^{3ix} + \bar{C}z\bar{z}^2e^{-ix} \\
&\quad +Cz^2\bar{z}e^{ix} + \bar{C}\bar{z}^3e^{-3ix} - Cz^3e^{3ix}e^{-iy'} - \bar{C}z\bar{z}^2e^{-ix}e^{-iy'} \\
&\quad -Cz^2\bar{z}e^{ix}e^{iy'} - \bar{C}\bar{z}^3e^{-3ix}e^{iy'} \\
&\quad -Cz^3e^{3ix}e^{-2iy'} - \bar{C}z\bar{z}^2e^{-ix}e^{2iy'} \\
&\quad -Cz^2\bar{z}e^{ix}e^{-2iy'} - \bar{C}\bar{z}^3e^{-3ix}e^{2iy'}
\end{aligned}
$$

Substituting ψ_1 and ψ_2 in (B.4) and using the expansions for $[\psi_1(x-y') - \psi_1(x)]^3$ and T , we then multiply both sides of B.4 by $\mathbf{1}$ and integrate w.r.to x to get $\Omega_3 = 0$. Next, multiply both sides by e^{-ix} and integrate with respect to x

$$
\begin{aligned}
0 &= z^2\bar{z}\int_0^{2\pi} A_3(y')\ [9e^{-iy'} + 3e^{iy'} - 3e^{-2iy'} - 9]\ dy' \\
&\quad +2C\ z^2\bar{z}\int_0^{2\pi} A_2(y')\ [e^{-iy'} - e^{iy'} - e^{-2iy'} + 1]\ dy' - g_2\alpha_1 z
\end{aligned}
$$

we can simplify this as follows

$$
0 = z^2\ \bar{z}[12B_1(A_3) - 3B_2(A_3) - 9B_0(A_3) + 2C\ B_0(A_2) - 2CB_2(A_2)] - g_2\alpha_1 z
$$

by letting $\zeta = 12B_1(A_3) - 3B_2(A_3) - 9B_0(A_3) + 2C\ B_0(A_2) - 2CB_2(A_2)$ and $\eta = -g_2\alpha_1$ we have the normal form at the bifurcation point as

$$0 \quad = \quad \zeta z^2 \bar{z} + \eta z$$

BIBLIOGRAPHY

[1] J. A. Acebrón, L. L. Bonilla, C. J. Pérez, F. Ritort and R. Spigler, *The Kuramoto Model: a simple paradigm for synchronization phenomena*, Reviews of Modern Physics 77(1) (2005) pp.137-185

[2] P. Ashwin and J. W. Swift, *The Dynamics of n Weakly Coupled Oscillators*, J. Nonlinear Sci. 2 (1992) pp.69-108

[3] M. Banaji, *Clustering in Globally Coupled Oscillators*, Dynamical Systems 17(3) (2002) pp.263-285

[4] T. Bem and J. Rinzel, *Short Duty Cycle Destabilizes a Half-center Oscillator,but Gap Junctions Restabilize the Anti-phase Pattern*, J. Neurophysiol. 91 (2004) pp.693-703

[5] T. Bem, Y. LeFeuvre, J. Simmers and P. Meyrand, *Electrical Coupling Can Prevent Expression of Adult-like Properties in an Embryonic Neural Circuit*, J. Neurophysiol. 87 (2002) pp.538-547

[6] C. Bou-Flores and A. J. Berger, *Gap junctions and Inhibitory Synapses Modulate Inspiratory Motoneuron Synchronization*, Neurophysiol. 85 (2001) pp.1543-1551

[7] E. Brown, P. Holmes and J. Moehlis, *Globally Coupled Oscillator Networks*, In: Perspectives and problems in Nonlinear Science: A celebratory Volume in Honor of Larry Sirovich, editors:E. Kaplan and J. Marsden and K. Sreenivasan, Springer, New York, (2003) pp.183-215

[8] C. C. Chow and N. Kopell, *Dynamics of Spiking Neurons With Electrical Coupling*, Neural Comp. 1 (1994) pp.313-321

[9] J. D. Crawford, *Amplitude Expansions for Instabilities in Populations of Globally Coupled Oscillators*, J. Stat. Phys. 74 (1994) pp.1047-1084

[10] J. D. Crawford, *Scaling and Singularities in the Entrainment of Globally Coupled Oscillators*, Phys. Rev. Lett. 74(21) (1995) pp.4341-4344

[11] J. D. Crawford and K. T. R. Davies, *The Behavior of Rings of Coupled Oscillators* , Physica D 125 (1999) pp.1-46

[12] E. Doedal, *AUTO: A program for the automatic bifurcation analysis of autonomous systems*, Congr. Numer. 30 (1981) pp. 265-284

[13] B. Ermentrout, J. W Wang, J. Flores and A. Gelperin, *Model for Transition from Waves to Synchrony in the Olfactory Lobe of Limax*, J. Comput. Neurosci. 17 (2004) pp.365-383

[14] G. B. Ermentrout and D. Kleinfeld, *Travelling Electrical Waves in Cortex:Inside from Phase Dynamics and Speculation on a Computational Role*, Neuron 29 (2001) pp.33-44

[15] B. Ermentrout, J. Flores and A. Gelperin, *Minimal Model of Oscillations and Waves in the Limax Olfactory Lobe with Tests of the Model's Predictive Power*, J. Neurophysiol. 79 (1998) pp.2677-2689

[16] B. Ermentrout, J. W Wang, J. Flores and A. Gelperin, *Model for Olfactory Discrimination and Learning in Limax procerebrum Incorporating Oscillatory Dynamics and Wave Propagation*, J. Neurophysiol. 85 (2001) pp.1444-1452

[17] G. B. Ermentrout and N. Kopell, *Inhibition-Produced patterning in Chains of Coupled Nonlinear Oscillators*, Siam J. Appl. Math. 54(2) (1994) pp.478-507

[18] G. B. Ermentrout, *Neural Networks as Spatio-Temporal Pattern-Forming Systems*, Rep. Prog. Phys. 12 (2000) pp.1643-1678

[19] G. B. Ermentrout, *Stable periodic solutions to Discrete and Continuum Arrays of Weakly Coupled Nonlinear Oscillators*, Siam J. Appl. Math. 52(6) (1992) pp.1665-1687

[20] G. B. Ermentrout, *The Behavior of Rings of Coupled Oscillators*, J. Math. Biology 23 (1985) pp.55-74

[21] Ermentrout, G.B *n:m Phase-Locking of Weakly Coupled Oscillators* J. Math. Biology 12, 327-342 (1981)

[22] B. Ermentrout, *Simulating, Analyzing, and Animating Dynamical Systems: A Guide to XPPAUT for Researchers and Students*, Software Environ Tools 14, SIAM, Philadelphia, 2002

[23] G.B. Ermentrout, *Stable small amplitude solutions in reaction diffusion systems*, Quart Appl Math, 39 (1981), pp.61-86

[24] B. Ermentrout, *Type I membranes, phase resetting curves, and synchrony*, Neural Comput. 8 (1996), pp. 979-1001

[25] G. B. Ermentrout and N. Kopell, *Multiple Pulse Interactions and Averaging in Systems of Coupled Neural Oscillators*,J. Math. Biol. 29(3) (1991) pp.195-217

[26] M. Galarreta and S. Hestrin *A network of Fast-spiking Cells in the Neocortex Connected by Electrical synapses*, Nature 402 (1999) pp.72-75

[27] D. Golomb, D. Hansel, B. Shraiman and H. Sompolinsky, *Clustering in Globally Coupled Phase Oscillators*, Phys. Rev. A 45(6) (1992) pp.3516-3530

[28] J. Guckenheimer, *Isochrons and phaseless sets*, J. Math. Biol. 1 (1975) pp.259-271

[29] F. Gurel Kazanci and G. B. Ermentrout, *Pattern formation in an Array of oscillators with Electrical and Chemical Coupling*, Siam J. Appl. Math. 67(2) (2007) pp.512-529

[30] D. Hansel, G. Mato and C. Meunier, *Phase Dynamics for Weakly Coupled Hodgkin-Huxley Neurons*, Europhys. Letters 23 (1993) p. 367

[31] D. Hansel, G. Mato and C. Meunier, *Clustering and Slow Switching in Globally coupled Phase Oscillators* Phys. Rev. E 48(5) (1993) pp.3470-3477

[32] D. Hansel, G. Mato, and C. Meunier, *Synchrony in excitatory neural networks*, Neural Comput, 7 (1995), pp. 307-337

[33] D. Hansel and G. Mato, *Existence and Stability of Persistent States in large neuronal networks*, Phys rev Lett, 86 (2001) pp. 4175-4178

[34] F. C. Hoppensteadt and E. M. Izhikevich, *Weakly Connected Neural Networks*, Springer, New York, 1997

[35] Izhikevich E. M. *Class 1 Neural Excitability, Conventional Synapses, Weakly Connected Networks, and Mathematical Foundations of Pulse-Coupled Models* . IEEE Transactions On Neural Networks,10:499-507 (1999)

[36] Izhikevich E. M. *Neural Excitability, Spiking, and Bursting*. International Journal of Bifurcation and Chaos. 10:1171-1266 (2000).

[37] Izhikevich E. M. *Subcritical Elliptic Bursting of Bautin Type*. SIAM Journal on Applied Mathematics, 60:503-535 (2000)

[38] Izhikevich E. M., *Dynamical Systems in Neuroscience:The Geometry of Excitability and Bursting*, Chapter 10, MIT Press, Cambridge, Mass., 2007

[39] N. Kopell, *Toward a Theory of Modeling Central Pattern Generators*, In: A Cohen, ed. Neural Control of Rhythmic Movements in Vertebrates, John Wiley, New York, (1998) pp.396-413

[40] N. Kopell and G. B. Ermentrout, *Phase Transitions and Other Phenomena in Chains of Coupled Oscillators*, Siam J. Appl. Math. 50(4) (1990) pp.1014-1052

[41] N. Kopell and G. B. Ermentrout, *Symmetry and Phaselocking in Chains of Weakly Coupled Oscillators*, Comm. Pure Appl. Math. 39 (1986) pp.623-660

[42] N. Kopell and B. Ermentrout, *Chemical and Electrical Synapses Perform Complementary Roles in the Synchronization of Interneuronal Networks*, Proc. Natl. Acad. Sci. 101(43) (2004) pp.15482-15487

[43] Y. Kuramoto, *Self-entrainment of a population of coupled nonlinear oscillators*, In: Proceedings of the international symposium on mathematical problems in theoretical physics, ed H. Araki, Lecture notes in physics 39, Springer, New York, (1975) pp.420-422

[44] Y. Kuramoto, *Chemical Oscillations, Waves and Turbulence*, Springer, Berlin, (1984)

[45] Yuri Kuznetsov, *Elements of Applied Bifurcation Theory*, Springer-Verlag, New York, 1998

[46] T. J. Lewis and J. Rinzel, *Dynamics of Spiking Neurons Connected by Both Inhibitory and Electrical Coupling*, J. Comput. Neurosci. 14 (2003) pp.283-309

[47] J. C. Neu, *Coupled Chemical Oscillators*, Siam J. Appl. Math. 37(2) (1979) pp.307-315

[48] K. Okuda, *Variety and generality of Clustering in Globally Coupled Oscillators*, Physica D 63 (1993) pp.424-436

[49] B. Pfeuty, G. Mato, D. Golomb and D. Hansel, *The Combined Effects of Inhibitory and Electrical Synapses in Synchrony*, Neural Comp. 17 (2005) pp.633-670

[50] J. Rinzel and B. Ermentrout, Analysis of Neural Excitability and Oscillations, Chapter 7 In: Methods in Neuronal Modeling: From ions to networks, C. Koch and I. Segev eds., MIT Press, Cambridge, MA, 1998

[51] H. Sakaguchi, *Cooperative Phenomena in Coupled Oscillator Systems under External Fields*, Prog. Theor. Phys. 79(1) (1988) pp.39-46

[52] H. Sakaguchi and Y. Kuramoto, *A soluble Active Rotator Model Showing Phase Transitions via Mutual Entrainment*, Prog. Theor. Phys.76(3) (1986) pp.576-581

[53] S. H. Strogatz, *From Kuramoto to Crawford: Exploring the Onset of Synchronization in Populations of Coupled Oscillators*, Physica D 143 (2000) pp.1-20

[54] S. H. Strogatz and R. E. Mirollo, *Stability of incoherence in a population of coupled oscillators*, J. Stat. Phys. 63 (1991) pp.613-635

[55] R. D. Traub, *Model of synchronized population bursts in electrically coupled interneurons containing active dendrites*, J. Comput. Neurosci. 2 (1995) pp.283-289

[56] C. van Vreeswijk and L.F. Abbott and G. B. Ermentrout, *When Inhibition not Excitation Synchronizes Neural Firing*, J. Comput. Neurosci. 1 (1994) pp.313-321

[57] M. A. Whittington, R. D. Traub, N. Kopell, B. Ermentrout and E. H. Buhl, *Inhibition Based Rhythms:Experimental and Mathematical Observations on Network Dynamics*, Int. J. Psychophysiol. 38 (2000) pp.315-336

[58] T. Williams, K. Sigvardt, N. Kopell, B. Ermentrout and M. Remler, *Forcing of Coupled nonlinear oscillators:studies of intersegmental coordination of the lamprey locomotor central pattern generator*, J. Neurophysiology. 64 (1990) pp.862-871

[59] A. T. Winfree, *Biological Rhythms and the behavior of populations of coupled oscillators*, J. Theor. Biol. 16 (1967) pp.15-42

[60] A. T. Winfree, *The Geometry of Biological Time*, Springer, New York, (1980)